

# Crystallizing membrane proteins using lipidic mesophases

Martin Caffrey<sup>1</sup> & Vadim Cherezov<sup>2</sup>

<sup>1</sup>Membrane Structural and Functional Biology Group, University of Limerick, Limerick, Ireland. <sup>2</sup>The Scripps Research Institute, Department of Molecular Biology, La Jolla, California, USA. Correspondence should be addressed to M.C. (martin.caffrey@ul.ie).

Published online 23 April 2009; doi:10.1038/nprot.2009.31

**A detailed protocol for crystallizing membrane proteins that makes use of lipidic mesophases is described. This has variously been referred to as the lipid cubic phase or *in meso* method. The method has been shown to be quite general in that it has been used to solve X-ray crystallographic structures of prokaryotic and eukaryotic proteins, proteins that are monomeric, homo- and hetero-multimeric, chromophore-containing and chromophore-free, and  $\alpha$ -helical and  $\beta$ -barrel proteins. Its most recent successes are the human-engineered  $\beta_2$ -adrenergic and adenosine A<sub>2A</sub> G protein-coupled receptors. Protocols are provided for preparing and characterizing the lipidic mesophase, for reconstituting the protein into the monoolein-based mesophase, for functional assay of the protein in the mesophase and for setting up crystallizations in manual mode. Methods for harvesting microcrystals are also described. The time required to prepare the protein-loaded mesophase and to set up a crystallization plate manually is about 1 h.**

## INTRODUCTION

High-resolution crystal structures of membrane proteins are in high demand for several reasons. Most immediately, they provide insight regarding the mode of action and, by extension, the physiological function of the protein at a molecular level. Such insight is often just the beginning of a long journey, as the crystal structure is the basis of a plethora of testable hypotheses of how the protein works and the nature of its interactions. Then there is the practical use to which such high-resolution structural information can be applied. This is best exemplified by structure-based rational drug design. One of the earliest examples of this is the viral membrane protein, neuraminidase. As soon as a crystal structure was available for the catalytic domain of the protein, the information was used to develop successful anti-flu drugs, such as Tamiflu and Zanamivir<sup>1</sup>. In the case of the G protein-coupled receptors, which are implicated in a host of diseases and are the target of many blockbuster drugs<sup>2</sup>, there are hundreds of slight structural variants that interact with a bewildering array of ligands. However, to understand and to exploit the structural basis for their individual specificities, high-resolution crystal structures are needed.

### An overview of protein crystallization methods

Membrane proteins can be crystallized for use in macromolecular crystallography by a variety of methodologies. These have been divided into two major groupings: the so-called *in surfo* and the bilayer methods<sup>3</sup>.

***In surfo* methods.** These methods make use of detergent- or surfactant-solubilized preparations directly in crystallization trials<sup>4</sup>. These take the form of vapor diffusion (both of the hanging- and sitting-drop type<sup>5</sup>), dialysis<sup>5,6</sup>, counter-diffusion<sup>7,8</sup> and microbatch<sup>9,10</sup> usually performed under oil. The primary advantage of the *in surfo* approach is that crystallization trials are set up using true solutions of protein detergent complexes that are relatively easy to handle. A long-cited problem associated with *in surfo* methods is the potentially destabilizing environment the protein finds itself in when dispersed in detergent micelles. Regardless of the hazards, the method, which is the first to have been

applied to membrane proteins, has proven successful with a wide range of membrane protein types (Membrane Protein Data Bank<sup>11</sup>, MPDB; <http://www.mpdb.ul.ie/>).

**Bilayer methods.** In contrast, these methods use a bimolecular lipid leaflet as the pad from which proteins launch into the crystal<sup>3</sup>. These include the bicelle, vesicle and the so-called *in meso* methods. The bicelle<sup>12</sup> and vesicle methods<sup>13</sup> have only recently been introduced and therefore have not been extensively tested or evaluated. However, both offer the advantage of being lipid bilayer-based in contrast to the *in surfo* method, which uses detergent micelles. The *in meso* method makes use of a lipidic mesophase (also known as a liquid crystalline phase), the cubic or sponge phase in particular, as the hosting medium and protein reservoir from which crystals grow. Similar to the bicelle and vesicle methods, it offers the advantage that the protein is removed from the potentially harmful environment of a detergent micelle. Furthermore, it is placed into a more familiar, hospitable, stabilizing and organizing lipid bilayer in and from which crystallogenesis takes place. The *in meso* method is the focus of this protocol.

### *In meso* crystallogenesis

*In meso* crystallogenesis takes place in and from a bicontinuous lipidic mesophase. It is important to appreciate that such mesophases are dynamic structures that respond to both compositional and environmental conditions in a sample history-dependent way. In the simplest case, composition refers to the relative amount of lipid and water in the system. However, under conditions of crystallogenesis, the system actually consists of an array of different components that can include protein, detergent, buffer, salt, hydrogen ions, polymers and small-molecule additives. Any and all of these can influence lipid-phase behavior, and it is most likely that the manner in which they do so influences the outcome of a particular crystallogenesis trial. It is important therefore to be familiar with the basic phase behavior of the hosting lipid with a view to understanding what is happening at a molecular, structural and a mesophase level at the various stages in crystallogenesis. For

this reason, a very brief introduction will be given here to the temperature–composition phase diagram of monoolein, the most successful lipid used to date for *in meso* crystallogenesi<sup>14</sup> (Fig. 1). At its simplest form, the phase diagram is a concise summary of phase propensity as water content and temperature are changed (see refs. 15,16 for useful background). The focus here is on the 20 °C isotherm, which is where the bulk of *in meso* crystallization has been performed (Fig. 1).

As noted, crystallogenesis begins with the cubic mesophase. The cubic mesophase is accessed in the monoolein/water system at 20 °C at an overall composition of about 40% (wt/wt) water (A in Fig. 1). This corresponds to the cubic phase of space group type Pn3m (cartoon representation of the phase is shown in Fig. 1). When additional water is added beyond the hydration limit of ~40% (wt/wt) water, it appears as a second phase and a two-phase system forms (B in Fig. 1). With reference to the crystallization trial, this corresponds to the cubic phase bolus sitting in an excess of precipitant solution. Moving along the 20 °C isotherm in the direction of reduced hydration, the next phase encountered after the cubic–Pn3m phase is a second cubic phase; this corresponds to the cubic phase of space group type Ia3d (C in Fig. 1). A continued reduction in water content triggers the formation of the lamellar liquid crystalline or L<sub>α</sub> phase (D in Fig. 1). The L<sub>α</sub> phase consists of planar lipid bilayers stacked atop one another and separated from each other by a layer of water. A further reduction in water gives rise to the lamellar crystalline or Lc phase, which is not liquid crystalline but a true solid (E in Fig. 1). Depending on how the lipid was treated thermally before manipulation, the system can at this point access what is referred to as the fluid isotropic phase, which, similar to the Lc phase, is not a mesophase but a true liquid. One final point of note regarding the phase diagram is that the excess hydration boundary shifts from about 50% (wt/wt) water at 0 °C to 25% (wt/wt) water at 85 °C. This temperature-induced shedding of water by the fully hydrated cubic mesophase is a useful diagnostic referred to later in this protocol.

That the method works and that it is a generally applicable method is no longer in doubt as evidenced by the statistics presented below. Less certain, however, is the mechanism by which it occurs. A hypothesis has been advanced for how the method works<sup>3</sup>, and convincing experimental evidence is available in support of the model (Fig. 2). The proposed mechanism begins with the target protein being solubilized in detergent from the parent biomembrane or from inclusion bodies. It is then purified using standard methodologies that include gradient centrifugation<sup>17</sup> and affinity<sup>18</sup>, ion exchange<sup>19</sup> and size-exclusion chromatographies<sup>20</sup>. The purified, concentrated protein in detergent solution

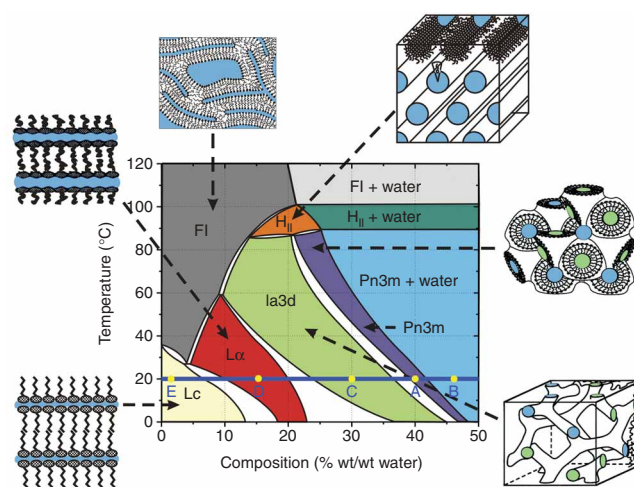


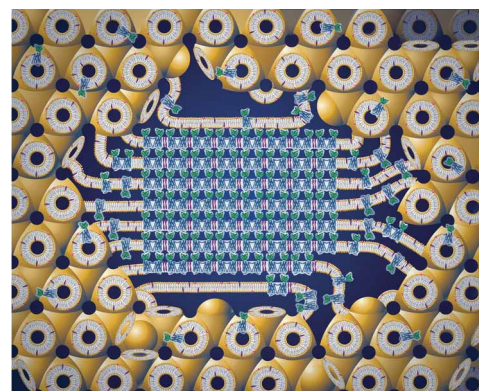
**Figure 1** | Temperature-composition phase diagram of the monoolein/water system determined under ‘conditions of use’ in the heating and cooling directions from 20 °C. Redrawn with permission from ref. 22. A cartoon representation of the various phase states is included in which colored zones represent water. The 20 °C isotherm is shown as a blue, horizontal line and points along it referred to in the text are labeled A–E. The liquid crystalline phases below ~17 °C are metastable<sup>14</sup>. Ia3d and Pn3m represent cubic phases.

is combined with lipid that, when fully hydrated, forms a viscous and sticky cubic mesophase. At this stage, the protein is considered to have been reconstituted into the bilayer of the cubic phase in a native and active conformation. The system is now destabilized by overlaying the mesophase with an excess of precipitant solution. The precipitant solution does not normally dissolve the cubic phase but exists as a separate liquid from which components diffuse into the mesophase bolus. The bolus can be considered as a molecular sponge with the lipid bilayer corresponding to the fabric of the sponge and the aqueous channels that permeate the mesophase corresponding to pores in the sponge. Components in the precipitant solution diffuse into the mesophase and trigger a series of phase transitions and separations, at least one of which leads to nucleation and growth of a protein crystal.

**Limitations of the *in meso* method**

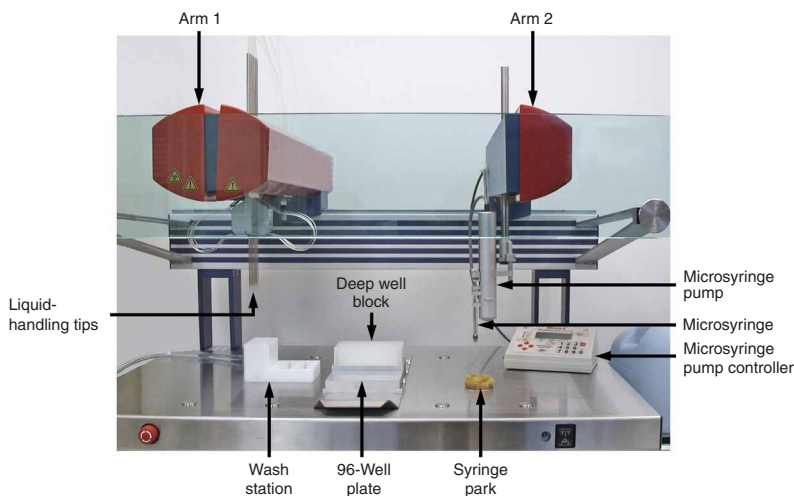
The *in meso* method was introduced over a decade ago<sup>21</sup>. Thus far, it is credited with 54 entries in the Protein Data Bank<sup>11</sup>, which

**Figure 2** | Cartoon representation of the events proposed to take place during the crystallization of an integral membrane protein from the lipidic cubic mesophase. The process begins with the protein reconstituted into the curved bilayers of the ‘bicontinuous’ cubic phase (tan). Added ‘precipitants’ shift the equilibrium away from stability in the cubic membrane. This leads to phase separation wherein protein molecules diffuse from the continuous bilayered reservoir of the cubic phase by way of a sheet-like or lamellar portal to lock into the lattice of the advancing crystal face (midsection of figure). Cocrystallization of the protein with native lipid (cholesterol) is shown in this illustration. As much as possible, the dimensions of the lipid (tan oval with tail), detergent (pink oval with tail), cholesterol (purple), protein (blue and green; β2AR-T4L; PDB code 2RH1), bilayer and aqueous channels (dark blue) have been drawn to scale. The lipid bilayer is ~40 Å thick.



## PROTOCOL

**Figure 3** | The *in meso* crystallization robot. The robot has two dispensing arms. Arm 1 includes four or eight tips and is used for handling liquid precipitant solutions. Arm 2 supports a microsyringe for dispensing the protein–lipid dispersion. The microsyringe dispenses mesophase by the action of a microsyringe pump, which in turn is driven by a controller. When not in use, arm 2 goes to a park position where the microsyringe needle tip is placed in a moist sponge. Also shown in the figure are a 96-well glass plate, a 96-deep-well block of precipitant solutions and a station where the tips on arm 1 are washed.



corresponds to about 10% of the integral membrane protein structures in the public domain. Our sense is that the yield of structures is not as high as it might be because the method has one major challenge: the cubic phase is extremely viscous (akin to a thick toothpaste) and sticky. As a result, it is not easy to handle with the tools commonly found in a biochemistry or a structural biology laboratory. Many have tried to use the method, but have abandoned it in frustration because the material at the heart of the method, the cubic phase, was found to be difficult to prepare and to dispense. The purpose of this protocol is to explain how to work with such mesophases and to provide simple and clear, step-by-step instructions for performing *in meso* crystallogenesis and related studies. The protocol is based on methods in routine use in the authors' laboratories and that have been used in characterizing and determining the high-resolution structures of the light-harvesting complex 2 from *Rhodospseudomonas acidophila*<sup>22</sup>, the outer membrane Vitamin B<sub>12</sub> transporter BtuB from *Escherichia coli*<sup>23</sup>, the outer membrane adhesin/invasin OpcA from *Neisseria meningitidis*<sup>24</sup> and the human  $\beta_2$ -adrenergic<sup>25</sup> and adenosine A<sub>2A</sub> (see ref. 26) G protein-coupled receptors (GPCRs). It is recommended that the initial trials (Steps 1–35) be performed with lipid and buffer in place of the target protein solution to gain familiarity with the method and with the unusually viscous and sticky nature of the mesophase.

### Automation of *in meso* crystallogenesis

*In meso* crystallogenesis can be done manually<sup>27</sup>, or robotically in high-throughput mode<sup>28</sup>. The former method is emphasized here because it can be done inexpensively and with materials and supplies that are readily available. We use the manual approach primarily for optimization trials that involve small numbers of samples. For high-throughput applications, we have built an *in meso* crystallization robot (Fig. 3), and a brief description of its use is included in Box 1. The robot offers distinct advantages, such as throughput, uniformity and the ability to perform the setup under what might be considered hostile conditions, such as in darkness and at low temperatures. It can also operate with extremely small volumes of protein (in the picoliter range) responding to the need to miniaturize to conserve valuable protein (and lipid). The steps that must be taken for such low volume setup are described in ref. 29.

### Overview of the procedure

The protocol is arranged by section using the procedural sequence followed in the laboratory for a typical crystallogenesis trial (Fig. 4). Crystallization plates are first prepared, and then the lipid–protein

## BOX 1 | ROBOTICS AND MINIATURIZATION

A huge compositional and environmental space must be explored to find conditions conducive to crystal growth. Having the crystallization and evaluation/scoring process automated allows for both rapid and high sample throughput. Some proteins have limited stability and the sooner they are included in crystallization trials the better. Accordingly, a robot allows for best use of available protein and lipid. Robotization, although not a guarantee of reproducibility, is more consistent with it than its manual alternative. Furthermore, robots do not suffer from fatigue and can be run continuously for extended periods unsupervised under hostile conditions, such as in the dark and at low temperatures.

We have built and implemented a unique, state-of-the-art robot for *in meso* crystallization (Fig. 3). The eight-tip variant operates with a setup rate of 96 wells per 6 min. It can also perform batch, vapor diffusion and bicelle crystallizations. A full description of the robot, its assembly, performance characteristics and use has been published<sup>28</sup> and is beyond the scope of this protocol.

The robot has been used to reduce the amount of protein (and lipid) required for a crystallization trial from a default volume of 50 nl to 530 pl of mesophase<sup>29</sup>. The latter corresponds to  $\sim 2$  ng protein for a 10 mg protein per ml stock solution. A description of how to exploit this feature of the robot has been reported<sup>29</sup>.

The high-throughput nature of the robot itself creates problems downstream at the crystallization trial evaluation stage. We have responded to this by moving toward high-throughput screen evaluation. The process has been robotized by digitally recording images of wells. In collaboration with a supplier of imaging equipment (Formulatrix), a system has been developed for *in meso* image archiving and processing for crystal detection and scoring. The imager has been customized to accommodate the low profile glass sandwich plates used for *in meso* crystallogenesis. The system available in the laboratory currently houses 1,000 *in meso* plates and 500 SBS-type plates with temperature control set at 20 °C. A smaller version of the instrument that houses 54 glass plates operates at 4 °C. Both instruments provide for recording images on a defined schedule at several positions across the 140- $\mu$ m-thick bolus in normal light and between crossed polarizers. Where images at multiple levels across the sample are recorded, a composite image can be created, which is useful at the visual inspection and evaluation stage.

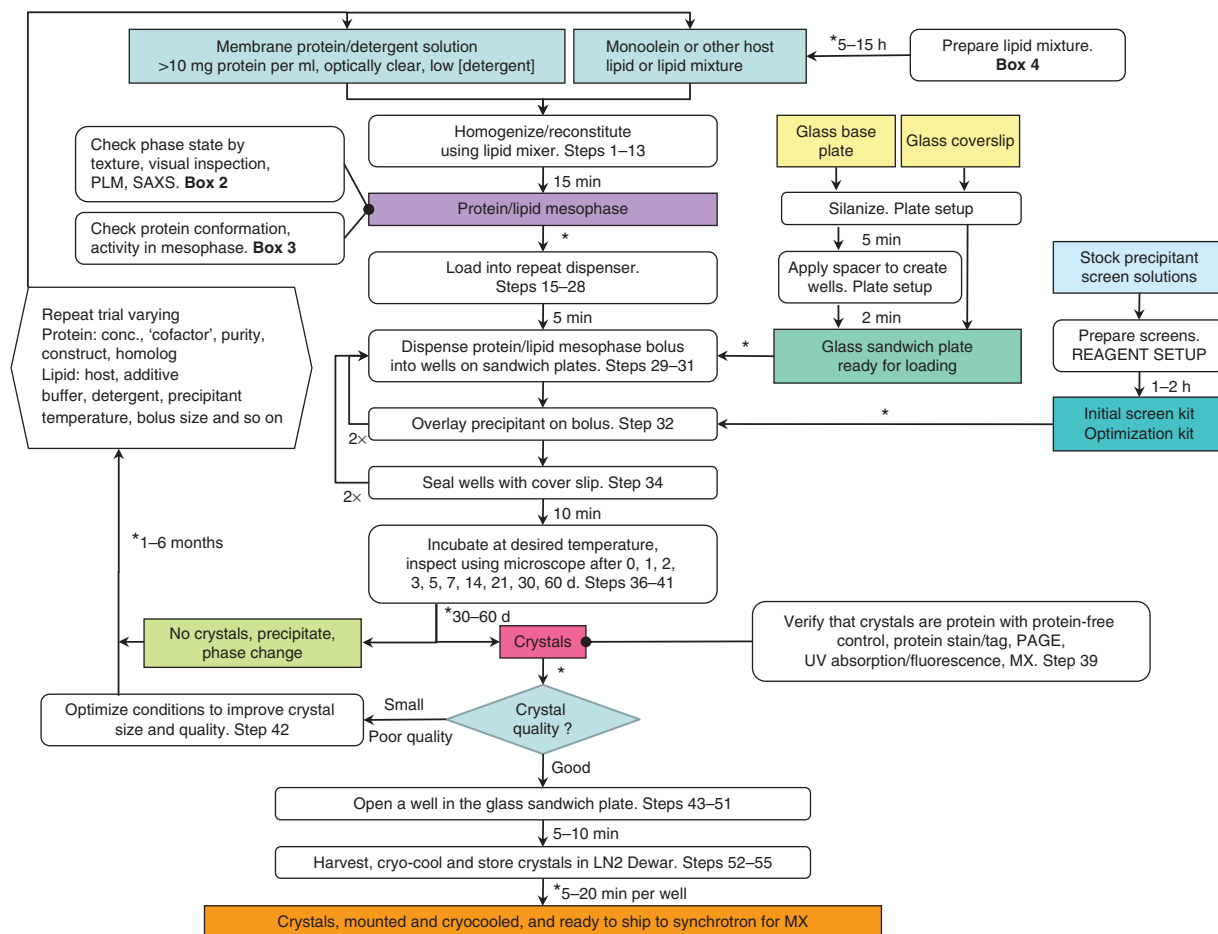


**Figure 4** | A flowchart summarizing the steps involved in and time required for setting up an *in meso* membrane protein crystallization trial. Boxed items represent starting and intermediate materials and products. Rounded boxes represent processes identified by step number(s) referred to in the text. Times are provided for the preparation of a single 27-well sandwich plate unless otherwise noted. Asterisks mark pause sites. 2× indicates that the procedure should be repeated twice.

mixing device is loaded and used to homogenize components. This enables the protein to reconstitute into the bilayer of the spontaneously formed cubic mesophase. Wells in crystallization plates are loaded with the protein-containing mesophase, which is then bathed in precipitant solution. The plates are sealed creating a glass sandwich of the mesophase, which offers unparalleled optical quality for subsequent imaging. Incubation and interrogation by normal and polarized light microscopy follow. Hits, when identified, are followed up with rounds of optimization that involve an exploration of incubation temperature, and precipitant and mesophase composition, which refers to lipids that create the hosting mesophase and to lipid additives. The next stage in the process involves harvesting crystals and is followed by diffraction measurements. As *in meso*-grown crystal can be small and in an opaque medium upon cryocooling, use is typically made of an X-ray synchrotron minibeam to locate and to orient the crystal ahead of data collection. The X-ray synchrotron minibeam is not covered in this protocol.

In addition to laying out the procedures for performing *in meso* crystallography and for crystal harvesting, this protocol includes methods that form part of the prescreening exercise, which is performed to minimize wasted time and effort with systems defective to begin with and that will not yield diffraction quality crystals. These include the following: methods used to characterize lipid purity and phase properties, including thin-layer chromatography, small-angle X-ray scattering and polarized light microscopy (Box 2), and a description of how the conformation and activity of the protein reconstituted in the cubic phase is evaluated by a variety of spectroscopies, including UV-visible, fluorescence and circular dichroism (Box 3). Prescreening and optimization should be performed by carrying out Steps 1–13 of PROCEDURE, followed by Boxes 2 and 3—taking care to set up the appropriate controls at relevant steps. When happy with the results of the analyses, carry out the crystallization experiment by repeating the PROCEDURE from Step 1 using the optimized conditions, continuing directly with Step 15.

**MATERIALS REAGENTS**

• Monoolein (1-oleoyl-*rac*-glycerol) (Sigma or Nu Chek) (refer to Box 2 for methods to characterize lipid purity and phase properties) ▲ **CRITICAL** The

monoacylglycerols used are unsaturated and can undergo oxidation. It is advised to always store stock lipid in the dark at as low a temperature as possible (–20 to –80 °C) in an inert atmosphere of nitrogen or preferably argon gas.



## BOX 2 | METHODS FOR CHARACTERIZING LIPID PURITY AND PHASE PROPERTIES

### 1. Thin-layer chromatography ● TIMING 2 h

Thin-layer chromatography (TLC) is used as a simple, sensitive and rapid method to determine lipid purity by the following protocol. TLC, as described here, can also be used very conveniently to identify and to quantify residual detergent and lipid in membrane protein preparations. Identification requires that standard reference detergents and lipids are available and loaded at Step 3.

#### Reagents

- Lipids for performing the TLC analysis
- Standard or reference lipids and detergents (Avanti Polar Lipids, Anatrace, Sigma)
- Organic solvents: chloroform, methanol, acetone, hexane, ethyl acetate, acetic acid, used to prepare mobile phases for TLC. All solvents should be of HPLC grade or higher purity ! **CAUTION** Most solvents are volatile and are irritants when inhaled or brought into contact with skin. Wear protective gloves and work in a ventilated hood.
- Sulfuric acid (Sigma, cat. no. 84733) ! **CAUTION** Sulfuric acid is a strong irritant and known carcinogen. Wear protective gloves and spray TLC plates in a specially designated spray box placed in a fume hood.

#### Equipment

- Alltec Adsorbosil Plus TLC plates (8–10 cm long, silica gel H, cat. no. 16385, Grace)
- Oven set at 110 °C
- Spotting Drummond Wiretrol micropipettes (Grace, cat. no. 3842)
- Atomizer reagent sprayer (Grace, cat. no. 17017)
- Cylindrical TLC tank (Grace, cat. no. 17108)
- Spray box (Grace, cat. no. 16408)
- Hot plate (Type 2600, Thermolyne)

#### PROCEDURE

1. Clean Adsorbosil Plus plates by prerunning them twice in chloroform/methanol (10/1 by vol) in a sealed chromatographic chamber. Prepare a plate for each solvent system to be used.
2. Dry the plates in an oven at 110 °C.
3. Spot 1, 5, 50 and 100 µg samples of lipid dissolved in chloroform about 1 cm from one end of the plate. Remove solvent by flushing the spot with a gentle stream of dry nitrogen gas.
4. Develop the plates to about 1 cm from the top of the plate using three different solvent systems: chloroform/acetone (96/4 by vol), chloroform/acetone/methanol/acetic acid (73.5/25/1/0.5 by vol) and hexane/ethyl acetate/acetone (73.5/1.5/25 by vol). Three solvent systems are used to move the lipid to different locations relative to the origin and the front.
5. Remove the plates and dry in air.
6. Visualize lipid spots by spraying the plate with a fine mist of 4.2 M sulfuric acid followed by charring on a hot plate at 250 °C in a fume hood. Lipid purity can be judged by comparing spot density and size at the different loadings with minor spots observed at the heavier loadings. For most lipids used in *in meso* crystallogensis studies, purity is in excess of 99%.

### 2. Phase characterization

A bicontinuous cubic or sponge phase is a requirement for *in meso* crystallogensis. However, there are many components in a crystallization mix that can affect mesophase stability. These include detergents, lipids, salts, polymers and solvents. It is important therefore to establish that the conditions under which crystallogensis is performed does not destroy the cubic phase. There are two methods that can be used for phase characterization, small-angle X-ray scattering (SAXS) and polarized light microscopy (PLM). The former provides definitive phase identification and microstructure quantization but requires specialized instrumentation. The latter is fast and simple but is less definitive than SAXS.

#### (A) Small-angle X-ray scattering ● TIMING 1–2 h

Phase characterization is carried out using small- and wide-angle X-ray diffraction as outlined in the following protocol.

#### Equipment

- X-ray quartz capillaries, 1 mm diameter (Hampton Research, cat. no. HR6-146)
- Capillary cutting stone (Hampton Research, cat. no. HR4-334)
- Propane/oxygen torch (The Little Torch, Smith Equipment)
- Crystaseal (optional) (Hawksley, cat. no. 01503-00)
- 5-minute epoxy (Hampton Research, cat. no. HR4-318)

#### PROCEDURE

1. Using a cutting stone, remove the flared open end of a 1-mm-diameter quartz capillary to create a tube of uniform diameter ~50 mm long and sealed at one end.
2. Transfer ~5 µl of mesophase sample (prepared as outlined in Steps 1–13 of the main PROCEDURE) to the bottom of the cut capillary using the lipid-mixing device and a 51-mm-long, 26-gauge transfer needle. Note that the sample used in this step can be prepared with an assortment of precipitant components, detergents, lipids and indeed proteins. The objective is to evaluate the compatibility of each test material, alone and in combination, as appropriate, with the *in meso* method. The main criterion used is that the test materials do not destabilize the cubic phase.

## BOX 2 | CONTINUED

3. Flame-seal the capillary using a propane/oxygen torch.

▲ **CRITICAL STEP** Seal the capillary at least 1 cm from the top of the mesophase using a small flame taking care not to dry, or worse, to char, the sample. Alternatively, use Crystaseal to seal the open capillary end instead of flame-sealing.

4. Apply a bead of 5-min epoxy to the sealed end of the capillary to protect and ensure the integrity of the seal.

■ **PAUSE POINT** If desired, samples can be stored at room temperature ( $\sim 20^\circ\text{C}$ ) for at least 1 d. In the presence of a mild dispersing medium where, for example, extremes of pH are avoided, samples in capillaries are stable for months at room temperature. If in doubt, degradation can be monitored by TLC as described above (**Box 2**, PROCEDURE 1).

5. Perform measurements using a rotating anode X-ray generator (Rigaku RU-300 operating at 45 kV and 250 mA) producing Ni-filtered Cu K $\alpha$  radiation (wavelength  $\lambda = 1.5418 \text{ \AA}$ ) as described<sup>50</sup>.

6. Measure sample-to-detector distance (25–35 cm) using a silver behenate standard<sup>51</sup> ( $d_{001}$ , 58.4  $\text{Å}$ ). The silver behenate can be loaded as a powder in a standard 1-mm-diameter X-ray capillary.

7. Mount the sample capillary in a temperature-controlled sample holder on the SAXS instrument and incubate for at least 4 h at  $20^\circ\text{C}$  before commencing the diffraction measurement. The temperature inside the sample holder is regulated by two thermoelectric Peltier effect elements controlled by a computer feedback system<sup>52</sup>. Measurements are performed at  $20.0 \pm 0.5^\circ\text{C}$ .

8. If the equipment setup permits, translate the samples continuously in the beam at a rate of  $2 \text{ mm min}^{-1}$  back and forth along a 2-mm section of the sample to average the contributions to total scattering from different parts of the sample and to minimize possible radiation damage effects<sup>53</sup>.

9. Record the diffraction pattern for about 30 min on high-resolution image plates or using a CCD or a single- or multiwire detector. X-ray-sensitive photographic film can also be used.

10. Process the diffraction data as described<sup>50</sup>. Phases are recognized by their characteristic X-ray diffraction patterns, a sampling of which is shown in **Figure 15**. In the wide-angle region of the pattern, scattering is diffuse and centered at  $\sim 4.6 \text{ Å}$  reflecting disordered chains that are the hallmark of liquid crystalline phases.

### (B) Polarized light microscopy ● TIMING 15 min

Mesophases have characteristic textures or appearances when viewed with a microscope using polarized light. This can be done very simply, rapidly and economically as follows.

#### Equipment

- Microscope glass slide, 1 inch  $\times$  3 inch (GoldSeal, cat. no. 3010)
- Glass coverslip, 22 mm  $\times$  22 mm (GoldSeal, cat. no. 3406)
- Microscope with polarizer and rotating analyzer

#### PROCEDURE

1. Using the lipid-mixing device (from Steps 1–13 of the main Procedure), place 1  $\mu\text{l}$  or less of the mesophase on a glass microscope slide and immediately cover it with a glass coverslip.

2. Examine the sample at room temperature at a magnification of  $\times 100$  in normal and between crossed polarized light. The cubic phase is nonbirefringent and will appear dark between crossed polarizers. The lamellar and hexagonal phases are birefringent with characteristic textures of the type shown in **Figure 8**. A gallery of PLM images recorded with an assortment of lipid/water systems is available for viewing on the Web (<http://www.caffreylabs.ul.ie/PLMWebsite/PLMPage.html>).

#### ? TROUBLESHOOTING



- Phospholipids, cholesterol (Avanti Polar Lipids) (refer to **Box 2** for methods to characterize lipid purity and phase properties)
- Crystallization screens (Hampton Research, Molecular Dimensions, Jena Biosciences, Qiagen, Emerald Biosystems)
- Chloroform ! **CAUTION** Toxic/irritant. Wear protective gloves and perform all manipulations under a fume hood.
- Methanol ! **CAUTION** Flammable/toxic. Wear protective gloves and perform all manipulations under a fume hood.
- Silanizing agent (e.g., AquaSil from the Pierce Division of Thermo Fisher Scientific, cat. no. 42799) ! **CAUTION** Flammable/irritant. Wear protective gloves and perform all manipulations under a fume hood.

#### EQUIPMENT

- Access to a microwave oven, hot running water or a small heating block that is stable at anywhere from  $40$  to  $60^\circ\text{C}$  is needed to melt the lipid
- Analytical balance with submilligram sensitivity
- Assortment of Eppendorf tubes and rack
- Eppendorf microcentrifuge capable of generating  $\sim 14,000g$
- Ultrasonic humidifier (optional)
- One 20–100  $\mu\text{l}$ , one 1–10  $\mu\text{l}$  and one 0.2–2  $\mu\text{l}$  adjustable pipette with disposable tips. We typically use Pipetman pipettes
- 10- $\mu\text{l}$  Hamilton gas-tight syringe with a removable needle (Hamilton, cat. no. 80065)

- Two 100- $\mu\text{l}$  Hamilton gas-tight syringes with a removable needle (Hamilton, cat. no. 81065)
- 25- $\mu\text{l}$  Hamilton gas-tight syringe with a removable needle (Hamilton, cat. no. 80265)
- Repeating dispenser (Hamilton, cat. no. 83700). Optionally, the dispenser can be modified, as described in ref. 30 to reduce the volume of cubic phase dispensed with a 10- $\mu\text{l}$  syringe from 200 to  $\sim 70 \text{ nl}$
- Two removable needles (gauge 22, Hamilton, cat. no. 7770-020) and two removable needle (RN) nuts (Hamilton, cat. no. 30902) to make a syringe coupler (see EQUIPMENT SETUP). Alternatively, the syringe coupler can be purchased commercially as part of the cubic LCP kit (Emerald Biosystems, cat. no. EBS-LCP-2). However, the critical threaded parts of this commercial coupler are made of plastic, whereas the original is made of steel and is extremely durable. We have not tested the commercial coupler and are not in a position to comment on its performance and/or suitability
- Short (0.375-inch), flat-tipped needle (point style 3, gauge 26, Hamilton, cat. no. 7804-03)

*Optional:* a desk lamp and a magnifying lens, to aid in viewing syringes, coupler and plates during loading and dispensing, are useful but not essential. A combined lamp/magnifying lens unit can also be used

## BOX 3 | EVALUATING PROTEIN CONFORMATION, DISPOSITION AND ACTIVITY IN MESO

Following the procedure outlined in Steps 1–13 of the main PROCEDURE, the assumption is that the protein has been reconstituted into the bilayer of the cubic phase. The model proposed (Fig. 2) posits that the reconstituted protein retains its native conformation and that it is functionally active. To evaluate this experimentally, the cubic phase must be prepared in a form that is optically isotropic, which, in turn, lends itself to investigation by a variety of spectroscopic techniques. These include electronic absorbance and fluorescence and circular dichroic spectroscopies<sup>23,24,42</sup>. Measurements are made in standard one-piece or sandwich glass or quartz cuvettes depending on the application; sandwich cuvettes are preferred when material is in short supply or when the protein concentration is high; quartz cuvettes are needed for measurements in the UV region.

### Equipment

- Removable needle, 21-mm-long, point style 3, 22-gauge (Hamilton, cat. no. 7804-01)
- Quartz cuvette, 3 mm path length (Hellma International, cat. no. 101.015)
- Quartz cuvette with detachable windows, 0.1 or 0.01 mm path length (optional) (Hellma, cat. no. 106) and holder (cat. no. 013.000)
- UV-transparent, disposable cuvette, path length 1 cm (BrandTech Scientific)
- Shaker (Mistral MultiMixer, Lab-Line instruments)
- Parafilm
- UV-visible spectrophotometer
- UV-visible fluorimeter
- CD spectrometer
- Centrifuge (e.g., Model MR 14.11, fixed angle rotor, Jouan). A swinging bucket rotor will work just as well.

### Loading standard one-piece cuvettes ● TIMING 10–20 min

Given the expense of the protein (and the lipid), spectroscopic measurements are usually done in the smallest volume cuvettes available that are compatible with data collection. Typically, we use 1 or 3 mm pathlength quartz cuvettes that can be used in both absorbance and fluorescence studies. Shims are used to raise the level of the cuvette in the holder to minimize the amount of mesophase required for the measurement. It is important, however, that the beam, which can be slitted down, at all times passes through the sample and that the air–mesophase interface is sufficiently distant from the beam to avoid scattering.

1. Load the protein-carrying mesophase (prepared as described in Steps 1–13 of the main PROCEDURE) into the cuvette from a 100- $\mu$ l Hamilton syringe with a 21-mm-long flat-tipped needle (point style 3, inner diameter, 0.41 mm; outer diameter, 0.72 mm; 22-gauge). Place the needle tip close to the base of the cuvette and slowly withdraw as the mesophase fills the cuvette.
2. Seal the cuvette tightly with multiple wrappings of Parafilm immediately after filling is complete. Occasionally, this process generates a uniform, optically transparent sample that fills the active area of the cuvette. In this case, the sample can be used directly for spectroscopic measurements.
3. Remove imperfections and bubbles that have become lodged in the sample by centrifuging the cuvettes for 10 min at 14,000g at room temperature.

▲ **CRITICAL STEP** To prevent the cuvette from breaking during centrifugation, a Teflon adapter has been machined that snugly holds the cuvette and that fits in the centrifuge tube (Fig. 16).

### Loading sandwich cuvettes ● TIMING 2–5 min

The 0.1- and 0.01-mm path length cuvettes used here consist of a front and a back window.

1. Place a small volume (approximately 1–10  $\mu$ l) of cubic phase (prepared as described in Steps 1–13 of the main PROCEDURE) on one of the windows in the region to be interrogated by the light beam.
  2. Immediately, make a sandwich of the mesophase by covering it with the second window. The two windows are held together in a spring-loaded cuvette adapter.
- ▲ **CRITICAL STEP** To ensure optical clarity, it is important to prepare the mesophase sample free of air bubbles and without excess buffer. This can be achieved by working with a mesophase at slightly less than full hydration and by avoiding trapped air at the mesophase mixing step (Steps 1–13). The sample is now ready for use for spectroscopic measurements.

### Analytical methods

For the range of spectroscopic measurements described below, it is recommended to prepare and to analyze samples in triplicate. If temperatures other than ambient are to be used, appropriate incubation times should be implemented to ensure that samples are fully equilibrated for spectroscopy. It should be noted that the supplementary analytical measurements presented below are not essential, nor indeed will they guarantee success at the crystallization stage. However, the more measurements that are made the more likely it is that problems will be detected before lengthy and costly crystallization trials are begun. Furthermore, the results of such measurements can provide insights into and a more rational approach for the crystallization of new membrane protein targets. If enough reconstituted mesophase is available, we recommend that electronic absorption and fluorescence spectra are recorded at a minimum. If a CD instrument is available, then dichroic measurements should also be made. All three spectroscopies report on different aspects of the conformation of the protein. In the case of proteins with chromophores, spectral properties can reflect the functional state of the protein. Ligand binding can be undertaken depending on the objectives and needs of the particular study.

### Analysis by UV-visible absorption ● TIMING 10 min

- (i) Place a protein-free mesophase-loaded cuvette in the sample holder of a dual-beam spectrophotometer. The reference holder is left empty. (Optional) If two matched cuvettes are available, it is possible to load one with protein-free mesophase to use as a reference and the other with protein-loaded mesophase to use as a sample. In this case, the absorption spectrum of the protein can be obtained directly with the reference and sample cuvettes in the reference and sample paths, respectively.
- (ii) Record the absorption spectrum in the appropriate range typically from 750 to 250 nm in 1-nm steps at 100 nm min<sup>-1</sup> with air as the reference.
- (iii) Repeat Steps (i) and (ii) using protein-loaded mesophase.
- (iv) Subtract the spectrum recorded in Step (ii) from that recorded in Step (iii) to obtain the absorption spectrum of the protein reconstituted in the mesophase.

### ? TROUBLESHOOTING

#### Analysis by fluorescence ● TIMING 10 min

- (i) Place a protein-loaded, square fluorescence cell in the cuvette holder of a fluorimeter.
  - (ii) Shim the cuvette to the proper height (see Fig. 16d).
  - (iii) Set the excitation wavelength to 305 nm. The latter is chosen to selectively excite tryptophan in the target protein with minimal contribution to recorded fluorescence from phenylalanine and tyrosine and to minimize photobleaching. As 305 nm is on the red edge of the tryptophan absorption peak, possible inner filter effects (Step (vii)) are lessened. Additionally, this wavelength is close to a peak in the Hg/Xe lamp emission spectrum at 302 nm, which provides for a stronger signal.
  - (iv) Record the emission spectra using 1-mm slits at the entrances to and exits from the excitation and emission monochromators providing an 8-nm band pass.
- ▲ **CRITICAL STEP** Emission spectra are typically recorded over a limited range from 360 to 320 nm (1 nm steps, 100 nm min<sup>-1</sup>) to minimize bleaching.
- (v) Repeat Steps (i–iv) using a protein-free mesophase reference sample.

## BOX 3 | CONTINUED

(vi) Subtract the spectrum obtained in Step (v) from that in Step (iv) to produce a spectrum corrected for background fluorescence from the nonprotein components of the sample.

(vii) If appropriate, correct for inner filter effect ( $I$ ), which occurs when sample absorption exceeds 0.1; fluorescence intensity no longer rises linearly with concentration, for all relevant data following established procedures<sup>54</sup>. Thus,

$$I = 10^{(A(\lambda_{\text{ex}}) + A(\lambda_{\text{em}}))/2}$$

where  $A(\lambda_{\text{ex}})$  and  $A(\lambda_{\text{em}})$  are the absorption of the sample at the excitation and emission wavelengths (see section Analysis by UV-Visible Absorption), respectively. The corrected fluorescence ( $F_c$ ) is calculated as:

$$F_c = IF$$

where  $F$  is the recorded fluorescence value.

### Analysis by fluorescence quenching ● TIMING 3–5 h

Quenching of tryptophan fluorescence by a lipid with a dibrominated acyl chain (bromo-MAG) can be used to investigate the disposition of the target protein in the cubic phase following a typical reconstitution protocol. If the protein resides in the bilayer, its intrinsic fluorescence will drop as the hosting, nonquenching lipid is replaced mole for mole by the bromo-MAG<sup>42</sup>. For this study, samples must be prepared where the mole fraction of bromo-MAG in the hosting MAG, e.g., monoolein, is varied from 0 to 1. The protocol used to prepare such lipid mixtures is described in **Box 4**. Alternatively, nitroxide-spin-labeled lipid can be used in place of the bromolipid for the quenching study<sup>55</sup>.

### Analysis by circular dichroism ● TIMING 10 min

The conformation of the target protein in detergent solution and that reconstituted into the lipidic cubic phase is determined conveniently by circular dichroism (CD). Spectra are recorded in the range from 250 to 190 nm in 1-nm steps with an equilibration time of 2 s per step using an AVIV circular dichroism spectrometer.

**▲ CRITICAL STEP** The bulk of the solution work is done using 1-mm path length quartz cuvettes of the sandwich type (see section Loading Sandwich Cuvettes). Because the lipid samples have high background absorbancies in the UV region (section Analysis by UV-Visual Absorption), the CD spectra can be noisy when collected using 1 mm cells. Accordingly, it is recommended that the bulk of the cubic phase data be collected using either 0.01 or 0.1 mm path length cuvettes, loaded as described above (section Loading Sandwich Cuvettes).

**Analysis by substrate/ligand binding.** As illustrated above, the lipidic mesophase, when properly manipulated, lends itself to interrogation by an assortment of spectroscopies. Accordingly, if the protein of interest undergoes a change in spectroscopic behavior during the course of an activity cycle, its functionality can be measured *in meso*. Thus, a change in electronic absorption or fluorescence, or CD upon ligand binding, can be used to quantify affinity. For this purpose, the ligand, if water-soluble, is combined with the protein solution at or before reconstitution and the spectroscopic signature is recorded as a function of total ligand concentration.

### (A) Measuring binding by ligand-induced quenching of intrinsic fluorescence ● TIMING 3–5 h

The following is a protocol for quantifying ligand-binding affinity based on a ligand-induced quenching of intrinsic fluorescence.

(i) Reconstitute the apoprotein into the cubic phase, as described in Steps 1–13 of the main PROCEDURE. Optionally, control data can be collected with the apoprotein in micellar solution for comparison with the *in meso* reconstituted protein.

(ii) Using mechanical mixing, combine the protein-loaded cubic phase with a solution containing ligand ranging in concentration both below and above the expected dissociation constant ( $K_d$ ) under conditions that ensure optical transparency. The latter can be achieved by adding a small amount of lipid to the mesophase after removing excess aqueous phase (see TROUBLESHOOTING to Step 13, main PROCEDURE).

(iii) Record the intrinsic fluorescence of the sample, as described in the section Analysis by Fluorescence.

(iv) Calculate  $K_d$  by Scatchard analysis. To this end, the fractional saturation of the protein with ligand ( $\nu$ ) is determined on the basis of a normalized fluorescence. Normalization is done using fluorescence values recorded in the absence of ligand and in the presence of saturating ligand concentration. Free ligand concentration,  $[L]_f$ , is calculated on the basis of the known total concentration of ligand and protein, and on  $\nu$ . A Scatchard plot of  $\nu/[L]_f$  versus  $\nu$  has an ordinate intercept of  $1/K_d$  and a slope of  $-1/K_d$  from which the binding constant is obtained. This analysis applies to a protein with a single ligand-binding site. We have used this approach to measure binding of vitamin B<sub>12</sub> to the cobalamin transporter, BtuB with a  $K_d$  of  $\sim 1$  nM (see ref. 23) and sialic acid to the adhesin, OpcA, with a  $K_d$  of  $\sim 1$   $\mu$ M (see ref. 24). The extent of quenching observed upon ligand saturation was  $\sim 30$  and  $\sim 10\%$ , respectively, for protein dispersed in the cubic phase.

### (B) Measuring binding by quantifying free ligand ● TIMING 3–7 d

It is possible to quantitate binding by monitoring the loss of ligand from a solution that has been equilibrated with the protein reconstituted into the lipidic cubic phase. Where the ligand has an absorbance in the UV-visible region, this can be done simply and directly in a cuvette using the following protocol, which has been successfully implemented for a water-soluble ligand with strong UV-visible absorption<sup>23</sup>. If the ligand is intrinsically fluorescent or carries a fluorescent tag or is radioactive, appropriate adjustments to the absorbance-based protocol can be made to quantify binding.

(i) Place a 30 mg bolus of protein-loaded cubic phase (60% (wt/wt) monoolein, 40% (wt/wt) buffer containing 1–20 mg protein per ml) on the bottom of a semimicro, UV-transparent, disposable cuvette (path length 1 cm).

(ii) Add 0.5 ml of ligand solution in a suitable buffer. The concentration of ligand used will depend on the  $K_d$ , its extinction coefficient at the interrogating wavelength ( $\lambda_i$ ), and the degree of saturation under investigation.

(iii) Tightly cap and seal the cuvette with Parafilm.

(iv) Shake the cuvettes gently while incubating at 20 °C. Other temperatures can be used in the range from 17 to 85 °C.

**▲ CRITICAL STEP** It is possible to screen at lower temperatures, but the experimenter must be aware that fully hydrated monoolein is not stable in the cubic phase below 17 °C (Step 38 of the main PROCEDURE; **Fig. 1**). If measurements are made in this temperature range, a conversion to the lamellar phase may occur unknown to the experimenter at any point during the incubation process. The issue of metastability has been discussed above (Step 38 of the main PROCEDURE).

(v) Monitor binding with elapsed time by recording the drop in the absorption of the bathing solution at  $\lambda_i$  nm using a spectrophotometer (see section Analysis by UV-Visible Absorption). Typically, equilibrium is reached after several days and is apparent as a leveling out in the concentration of ligand in the bathing solution above the mesophase. If the ligand is colored, binding can also be observed as a coloration of the mesophase at the bottom of the cuvette (see **Fig. 17d**). Control samples containing the ligand buffer with and without protein-free cubic phase should be monitored for a change in the absorption at  $\lambda_i$  over the same equilibration period. For water-soluble ligands, mesophase binding is usually negligible. The more lipophilic the ligand, the greater this background will be.



## PROTOCOL

- Microscope slides, 1 inch × 3 inch (GoldSeal, cat. no. 3010)
- Microscope coverslips, 1 inch × 1 inch (Fisher Scientific, cat. no. 12-548C)
- Perforated double stick spacer (3M 9500PC double stick tape, 0.140 mm thick, 5-mm-diameter holes, 27 holes in total, 7 mm spacing between holes, overall size 1 inch × 3 inch. The arrangement of holes in the 27-well plate is shown in **Figure 5** (see also ref. 27). Spacers with punched holes can be obtained from a die-cutting company, such as Saunders Corporation)
- Two wash bottles with fine tips. One filled with milli-Q or distilled water, and the other with methanol. These are used to clean the syringes, needles and coupler. Methanol is used first, then water
- Gloves to protect hands while working with organic solvents
- Pressure-regulated air or nitrogen gas with a hose and a fine tip for drying syringes, needles, ferrules and coupler. A can of pressurized air works well
- Parafilm, 1 cm × 1 cm and 1 inch × 1 inch squares
- Detergent-binding materials, such as Bio-Beads SM-2 (Bio-Rad, cat. no. 152-3920)
- Hand-held roller or brayer (Fisher Scientific, cat. no. 50820937)
- Tools for harvesting crystals from glass *in meso* crystallization plates:
  - Hampton glass cutting stone, broken to present a fresh, sharp edge (Hampton Research, cat. no. HR4-334)
  - Fine point tweezers (Ted Pella, cat. no. 510)
  - Probing tool with a sharp point angled at 45 degrees (Ted Pella, cat. no. 13650)
- *In meso* crystallization plate with protein crystals
- Precipitant solution for the condition that supports crystal growth
- Stereomicroscope with crossed polarizer capability, magnification range ×20–100 and with a large operating distance (>60 mm) for easy access to plate and for ease in harvesting crystals
- Pipette with tip set to 5 µl for transferring the precipitant solution
- Magnetic wand (Hampton Research, cat. no. HR4-729)
- Covered Dewar (Hampton Research, cat. no. HR4-673) filled with liquid nitrogen
- Storage or shipping Dewar (Taylor-Wharton)
- *Magnetic caps*: standard and advanced light source (ALS)-style caps are available from Hampton Research; SPINE-style caps are available from Molecular Dimensions and Hampton Research. Check with your beamline host for acceptable cap styles
- *Cryoloops*: for harvesting small crystals from lipidic cubic phase, we recommend MicroMounts with 20–50 µm aperture, available from MiTeGen (cat. nos. M1-Lxx-20, M1-Lxx-30 and M1-Lxx-50) ([http://mitegen.com/mic\\_catalog.php?c=MicroMounts](http://mitegen.com/mic_catalog.php?c=MicroMounts)). Alternatively, nylon cryoloops can be obtained from Hampton Research or LithoLoops can be purchased from Molecular Dimensions. Check with your beamline host for acceptable pin lengths
- Super Glue (Hampton Research, cat. no. HR4-316) or an Epoxy (Hampton Research, cat. no. HR4-318)
- *Optional*: Puck to house multiple mounted crystals. These are typically used with automounters. However, some pucks, such as ALS-style pucks, are also convenient for manual mounting (ALS-style pucks and accessories can be purchased from Boyd Technologies; SSRL cassette and Unipucks can be purchased from Crystal Positioning System; Rigaku-style pucks can be purchased from Rigaku; EMBL/ESRF pucks and accessories are available from Molecular Dimensions). Check with your beamline host for puck styles that are compatible with their automounter
- *Optional*: cryovials for manual mounting (Hampton Research, cat. no. HR4-731). Some automounters, such as Rigaku and EMBL/ESRF, require cryovials (CrystalCap HT from Hampton Research; SPINE style magnetic cryovials from Molecular Dimensions)
- *Optional*: CrystalCap holder (Hampton Research, cat. no. HR4-707) is used to hold cryovials in the Dewar during crystal harvesting
- *Optional*: CryoCane (Hampton Research, cat. no. HR4-709 or HR4-711) and CryoSleeve (Hampton Research, cat. no. HR4-708) are used for storing and transporting mounted crystals in Cryovials

### REAGENT SETUP

**! CAUTION** Many of the reagents used in crystallogensis are toxic, and instructions for handling, as described on the relevant Materials Safety and Data Sheets, should be followed. **▲ CRITICAL** Preformulated buffers, precipitants (salts, polymers, volatile and nonvolatile organic solvents), detergents, surfactants, additives, reducing agents and ligands required for the solutions mentioned below are available commercially (see websites for Hampton Research, Molecular Dimensions, Jena Biosciences, Qiagen, Emerald

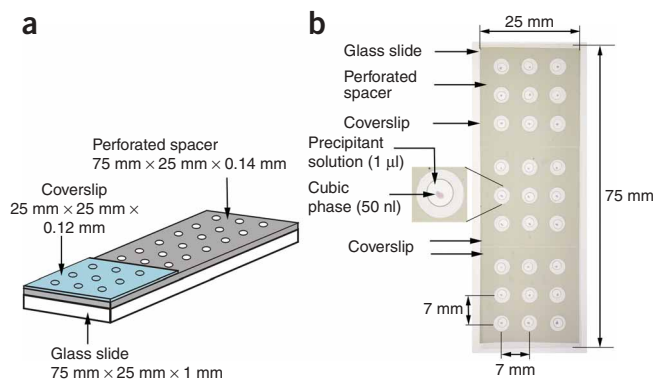


**Figure 5** | The glass sandwich crystallization plate. **(a)** A perspective drawing of the plate consisting of a glass slide base, a perforated spacer and a glass coverslip. **(b)** A photograph of a 27-well plate viewed from above where each well is loaded with 1 µl of a precipitant solution and 50 nl of cubic phase containing bacteriorhodopsin. The plate has three coverslips in place. Adapted from ref. 27.

Biosystems, Sigma-Aldrich and so on). These reagents are used to prepare various buffers and precipitant cocktails. The different sources vary in the range of ingredients, concentrations and volumes provided. Refer to the manufacturer's instructions for maximum storage time and preferred storage conditions of light and temperature. **▲ CRITICAL** Reproducible crystallogensis benefits from the use of materials of the highest and most uniform quality and purity. **Membrane protein solution** The target protein should be solubilized in detergent, purified and concentrated preferably to higher than 10 mg of protein per ml. It is advisable to work with a protein sample that is monodispersed as judged, for example, by analytical size exclusion chromatography or light scattering. Extensive purification can lead to loss of a critical lipid (and other components) from the protein that can compromise the production of diffraction quality crystals. If this occurs, it may be necessary to add lipid back to the protein solution or to supplement the hosting mesophase with membrane lipids (see **Box 4**) for successful crystallization. Most of the common detergents are compatible with the *in meso* crystallization approach when used at typical concentrations of a few times the critical micelle concentration. Care should be taken, however, to minimize the detergent content in the concentrated sample because high levels of detergents can destroy the lipidic cubic phase and transform it entirely into a lamellar phase (see refs. 31,32). If the protein cannot be concentrated to  $\geq 10 \text{ mg ml}^{-1}$  in solution, it is still possible to work with dilute samples and to increase the protein content of the lipidic cubic phase during the mixing stage, provided the concentration of detergent is not too high (see Step 13 of PROCEDURE).

### EQUIPMENT SETUP

**Syringe coupler** Most of the equipment needed to perform *in meso* crystallogensis is available commercially. The one exception is the syringe coupler. This simple device (**Fig. 6**) allows two Hamilton syringes to be combined for use in mixing, homogenizing and dispensing viscous lipid dispersions with minimal dead volume. The design and performance specification of the device have been published along with machining blueprints for use in construction<sup>33</sup>. The coupler can be fabricated at most home institutions using commercially available parts (two removable needles (gauge 22) and two RN nuts), access to a machine shop and the instructions in ref. 33. Further details regarding the syringe coupler are available from M. Caffrey on request.

**Choice of crystallization plates** Best optical quality is guaranteed when *in meso* crystallogensis is performed in glass sandwich plates, as described in Steps 15–35 of PROCEDURE. However, there are situations where commercial plates, typically for hanging-drop vapor diffusion and microbatch trials, can be used to advantage (**Fig. 7**). In this case, loading is still achieved as described in Steps 15–35 of PROCEDURE. Visualization, particularly of small colorless crystals within the mesophase bolus, can be hampered, however, as a result of the mesophase surface becoming wrinkled and light-scattering when in direct contact with the precipitant solution. This can be circumvented in the microbatch plates by placing a 5-mm-diameter glass coverslip on top of the bolus, thereby creating a sandwich of the mesophase between the base of the well and the coverslip. In

**BOX 4 | PREPARING LIPID MIXTURES WITH MONOLEIN AS THE HOST ● TIMING 5–15 h**

1. Weigh ~100 mg of monoolein in a small amber glass vial with a Teflon-lined cap.
2. Add an appropriate amount of a second lipid (typically 10–20 mol% second lipid, 90–80 mol% monoolein) by weighing it on a small piece of weighing paper or aluminum foil and transferring it to the vial.  
**▲ CRITICAL STEP** Most lipids are hygroscopic and are prone to oxidation. Store stock lipids at –20 °C. Do not open the sealed vial containing the lipid until it has warmed to room temperature after taking it from the freezer. Minimize the time spent manipulating the lipids after removing them from storage vials. As soon as possible, flush the vial with dry nitrogen or argon gas before closing and sealing with Parafilm for storage at low temperature and in the dark.
3. Dissolve the monoolein and the second lipid in ~500 µl of chloroform/methanol (2/1 by vol). Mix to create a homogenous solution.
4. Remove bulk organic solvent with a gentle stream of nitrogen gas and make a thin shell of the lipid on the bottom of the vial as it dries. Keep the vial warm during solvent evaporation to facilitate the process. This can be done simply by holding the base of the vial between your fingers while rotating it in the stream of nitrogen gas.
5. Remove the last traces of solvent by placing the open vial under vacuum (~50 mTorr) for a minimum of 4 h. It is preferable to do this overnight.
6. Flush the vial with dry argon gas. Close the cap tightly and secure it with Parafilm. This lipid mixture can now be used in place of monoolein in Step 5 of the main PROCEDURE.  
**■ PAUSE POINT** Store for up to 1 year at –20 or –80 °C.

hanging-drop plates, the bolus can effectively be similarly sandwiched as illustrated in **Figure 7**. When working with commercial plates, those made from low birefringency plastic should be used for best viewing and imaging of crystal growth using polarized light microscopy (PLM).

**Plate setup for crystallization** ● **TIMING** 5–10 min per plate) Silanize standard microscope slides and coverslips; use a commercially available silanizing solution and follow the protocol specified by the supplier. Remove the protective paper cover from one surface of a strip of perforated double stick spacer tape (3 wells wide and 9 wells long). Place the tape, exposed sticky surface down, in contact with the surface of a silanized microscope slide. Pressure-seal the tape to the slide using a brayer. Aluminum foil can be placed between the tape and the roller to protect the base of the wells. Remove the second protective paper cover from the spacer tape to expose its upper sticky surface. This procedure generates a 27-well glass plate that is ready for loading and

subsequent sealing (**Fig. 5**). Place individual silanized coverslips in a row in close proximity to the plate for fast and efficient sealing of wells as soon as loading is complete. **▲ CRITICAL** Plates can be prepared in advance and stored for several weeks at room temperature (20–23 °C) in a clean, sealed container.

**Micromounts** Attach micromounts with a suitable pin length to magnetic crystal caps using a Super Glue or an Epoxy. The base of the cap must be clearly labeled so the crystal can be identified later at the synchrotron. Before MiTeGen Micromounts became available, nylon cryoloops (Hampton Research) were used to harvest crystals. This was not easy, given the stiffness of the cubic phase and the flexibility of the cryoloops. Oftentimes, a microprobe (Hampton Research) or an acupuncture needle was used to work a crystal out to the surface of the mesophase for more facile harvesting with the cryoloop. Micromounts from MiTeGen are considerably more stiff and can be used to fish and to harvest, although some of the fishing can be done with microtools.

**PROCEDURE**

**Loading the lipid mixer ● TIMING 10 min**

- 1| Remove the lipid, monoolein, from the freezer and allow it to adjust to room temperature.  
**▲ CRITICAL STEP** Monoolein and other monoacylglycerol lipids are hygroscopic. Therefore, allow for full equilibration to room temperature before opening the container.
- 2| Disconnect the needle and remove the Teflon ferrule from two 100-µl Hamilton gas-tight syringes.
- 3| Weigh both syringes with plungers in place.
- 4| Remove the plunger from one of the syringes.
- 5| With a fine-tipped spatula, work about 10–30 mg (approximately 10–30 µl, density of monoolein at 20 °C is 0.942 g cm<sup>-3</sup>, see ref. 34) of the waxy lipid (or lipid mixture; see **Boxes 4** and **5**) into the open end of the syringe. Return the plunger to the barrel and place the syringe in an oven at about 37 °C to melt the lipid. Alternatively, the lipid can be melted before loading into the syringe. In this case, a 20- or 200-µl pipette with a standard disposable tip is used to remove 10–30 µl of the molten lipid and to place it in the barrel of the syringe (plunger removed) from the plunger end. Return the plunger to the barrel, at which point its Teflon tip will make contact with the molten lipid. With the syringe held vertically, barrel termination end up, move the plunger slowly up the barrel along with the molten lipid; this will usually lead to air locks and bubbles being removed from the lipid. Ideally,

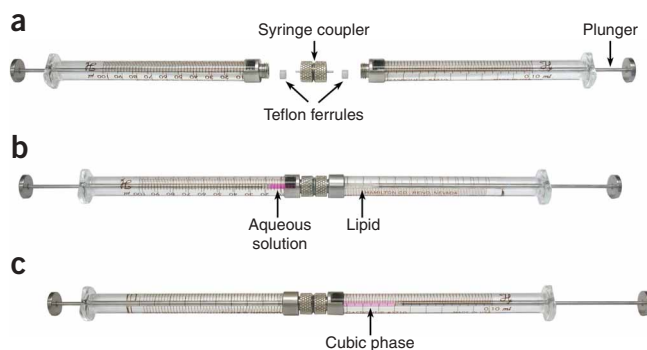


**Figure 6** | The lipid-mixing device. The coupled syringe mixer is shown (a) disassembled and (b,c) assembled. In (b), the mixer is shown loaded and ready for mixing with lipid (white) in one syringe and protein solution (pink) in the other. The homogenized, protein-loaded mesophase (light pink) in the syringe on the right is shown in (c).

## PROTOCOL

one ends up at this stage with a continuous volume of molten lipid in direct contact with the Teflon tip of the plunger. In this case, the volume of lipid in the syringe can be read directly from the  $\mu\text{l}$  markings on the barrel. Given that monoolein has a density of  $0.942 \text{ g ml}^{-1}$  (see ref. 34), the weight of lipid in the syringe can be calculated from the recorded volume. Alternatively, the loaded syringe can be reweighed and the lipid mass obtained by taring.

**▲ CRITICAL STEP** Incubate the lipid for just long enough to melt the lipid for easy handling. Extensive heating can lead to lipid degradation.

**6|** Attach the coupler, with both ferrules in place, to the open end of the lipid-loaded syringe. Carefully screw the coupler into position.

**▲ CRITICAL STEP** The coupler must be tightened to a degree that the syringe contents do not leak under the pressure of mechanical mixing but not overtightened, which can deform the ferrule and/or break the glued seal between the glass barrel and the steel barrel termination, resulting in leakage during mixing.

**7|** Use the plunger to force the molten lipid up the barrel and slowly and gently into the narrow bore needle at the core of the coupler. If the needle is slightly overfilled, the lipid will be seen beading out at its open end. By backing up the plunger slightly, the excess lipid can be withdrawn into the coupler until it is just flush with the tip of the coupler needle. In this case, the syringe/coupler unit is fully loaded and ready to be combined with the protein solution-loaded syringe at Step 12.

**8|** Calculate the volume of protein solution that can/should be used to form the cubic phase at or close to full hydration. For monoolein at  $20^\circ\text{C}$ , full hydration with water occurs at close to  $\sim 40\%$  (wt/wt) water<sup>14</sup> (**Fig. 1**). Thus, for example, if the weight of lipid in the lipid-loaded syringe is 21 mg, then  $((21/3) \times 2 = )$  14 mg, corresponding to  $\sim 14 \mu\text{l}$ , of protein solution will be required.

**9|** Centrifuge the protein solution in a 0.5-ml Eppendorf tube at  $14,000g$  for 5–10 min at  $4^\circ\text{C}$  to remove large aggregates before setting up crystallization trials.

**▲ CRITICAL STEP** The amount of detergent in the protein solution used for *in meso* crystallization trials should be minimized to avoid destabilizing the bicontinuous mesophase (see also Troubleshooting section).

**10|** The second 100- $\mu\text{l}$  Hamilton syringe is used to house the protein solution (or control solution required for prescreening analyses; see **Box 3**). Withdraw the plunger in the syringe to the 20–30  $\mu\text{l}$  mark and slowly inject 14  $\mu\text{l}$  of protein solution

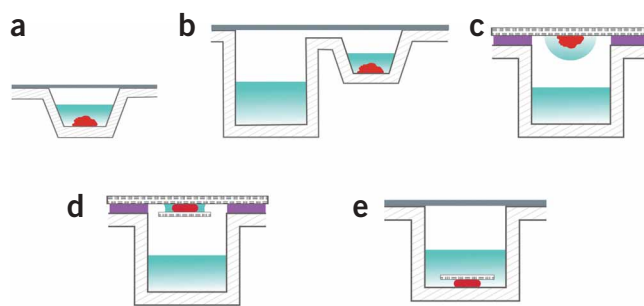


**Figure 7 |** Ways to set up *in meso* crystallization trials using commercial plates. The types of plates used include (a) microbatch, (b) sitting drop and (c,d) hanging drop. In d and e, a sandwich is made of the mesophase (red) by placing a small glass coverslip (hatched) (d) below or (e) above the bolus. The precipitant solution is colored a shaded pale blue, the vacuum grease is purple and the sealing tape is gray.

## BOX 5 | OPTIMIZING CRYSTALLOGENESIS

The conditions to be optimized for *in meso* crystallogeneses are, by and large, those implemented with soluble and membrane proteins by the more standard vapor diffusion and batch techniques. These include buffer, salt, polymer and additive type and concentration, as well as pH and temperature (see **▲ CRITICAL STEP** at Step 36 regarding temperature). In addition to these more standard approaches, optimization *in meso* can also be implemented at the level of the composition of the lipid bilayer from which nuclei form and crystals grow. Thus, the identity of the lipid used to form the cubic phase can be changed or a lipid additive can be included. In the former case, there are several alternative monoacylglycerols to monoolein, the default lipid, that are available commercially (e.g., from Nu-Chek Prep Inc.) and that can be used. These include monopalmitolein and monovaccenin. To augment this effort, we have a lipid synthesis and purification program in place in the laboratory and several novel monoacylglycerols have proven useful at the screening stage<sup>35,56</sup>. From a practical perspective, these alternative lipids are used in exactly the same way as has been described in Steps 1–13 for the default lipid monoolein.

When an additive lipid is to be included as part of the optimization process, care must be taken to ensure that the amount added to the hosting lipid does not destabilize the cubic phase. We have investigated this for several lipids and found that the cubic phase of monoolein can accommodate up to 20 mol% DOPE, 20 mol% DOPC, 25 mol% cholesterol, 5 mol% DOPS and 7 mol% cardiolipin<sup>57</sup>. In that study, phase identification and microstructure characterization were performed using small-angle X-ray scattering (**Box 2**). However, optical clarity and texture between crossed polarizers, as described in **Box 2**, are other less-demanding but less-definitive ways of making this determination. A protocol for preparing such lipid mixtures, with monoolein as the host, is described in **Box 4**.

It should be noted that several membrane proteins have lipophilic cofactors and ligands and their mode of interaction with the target can be of interest. They can also stabilize the protein and render the complex more crystallizable. Such ligands can be combined with the lipid before cubic-phase preparation in the same way that lipid additives are incorporated, as described in **Box 4**.

onto the Teflon tip of the plunger using a 25- $\mu$ l Hamilton gas-tight syringe fitted with a 26s gauge, flat-tipped (point style 3) needle.

**▲ CRITICAL STEP** Every effort should be made to avoid trapping air bubbles in the delivered protein solution because removing them after loading can be difficult given the tendency of such detergent-containing solutions to foam. If moving the plunger up and down in the barrel while holding the syringe in a vertical position does not eliminate trapped bubbles, it is best to start again. To this end, aspirate the protein solution from the syringe, transfer it back to an Eppendorf tube and centrifuge as in Step 9.

**11|** At this stage, the protein solution should exist as a homogenous, clear solution in direct contact with the Teflon tip of the plunger. Determine the volume of the protein solution by reading the  $\mu$ l markings on the syringe barrel, which should match the volume loaded initially. This is usually the case. Alternatively, the loaded syringe can be reweighed and the weight of the protein solution can be calculated by taring. In preparation for combining with the lipid-loaded syringe, carefully inch the protein solution up the barrel to end up flush with its open end. This can be observed by looking down through the barrel termination end. A table lamp and magnifying lens are a great help at this step.

**12|** The lipid- and protein solution-loaded syringes are now ready to be combined in preparation for mixing. To do this, screw the protein syringe into the open end of the coupler attached to the lipid syringe. Having combined the two syringes by way of the coupler, a continuous volume of liquid should exist from lipid in one syringe through the coupler to protein solution in the other syringe. In preparation for mixing, the assembled unit is held with one syringe in the right hand and the other in the left. Torque is applied to both barrels through to the coupler using the fingers and thumb of both hands to ensure that the seal against the ferrules in the coupler remains intact.

**▲ CRITICAL STEP** Overtightening the assembled mixing device at this stage will damage the ferrules and cause leaking. Undertightening will also lead to leaking. It is a matter of experience, with the inevitable trial and error and occasional loss of sample. It is worthwhile therefore practicing with lipid and water or buffer solution to get a feel for the system before launching into using valuable protein solution.

#### Mixing lipid and protein solution: making the mesophase ● TIMING 5 min

**13|** To effect mixing, advance the plunger on the protein side of the assembled mixing unit to its limit, with the thumb or index finger driving the protein solution out of the protein syringe, through the coupler and into the lipid syringe. If the unit has been sealed effectively, this action will cause an equal and opposite movement of the plunger on the lipid side. The plunger on the lipid side is now used to drive the contents of the lipid syringe back through the coupler and into the protein syringe. The process is repeated many times; occasionally, a hundred passages or more are required to produce a homogenous mesophase.

**▲ CRITICAL STEP** At the start of mixing, movement of material back and forth through the coupler can be uneven and, at times, extra force is needed to effect mixing. This is to be expected as different mesophases come and go in the course of the homogenization and hydration process. Refer to the 20 °C isotherm in **Figure 1** for the phases that are likely to form in the process. Initial mixing is usually accompanied by the development of a nonuniform cloudiness in the sample and is expected. As homogenization progresses, the texture, as sensed by the force needed to move the plungers back and forth, becomes more uniform and characteristic of the viscous cubic phase, as does the visual appearance of the emerging cubic mesophase (which is optically clear).

**▲ CRITICAL STEP** If the concentration of the protein solution is low (e.g., less than 5 mg ml<sup>-1</sup>), then using an excess of it at this stage can be useful because the protein will preferentially partition into the lipidic mesophase. In this way, the protein concentration in the actual cubic phase can be increased. In practice, a two- to fivefold increase in concentration is achievable depending on the detergent concentration in the initial protein sample. The bulk of the excess (protein-free) buffer that spontaneously separates from the fully hydrated mesophase can be easily removed by uncoupling the mixing unit and retrieving excess liquid using a separate Hamilton syringe. A small amount of the excess buffer, however, will inevitably become trapped in the mesophase and this will contribute to diluting the precipitant solution added later in the process (Step 32). Therefore, it is advisable to add a few microliters of lipid at this stage and to mix to homogeneity to absorb the excess buffer.

**▲ CRITICAL STEP** If conditions are appropriate and the cubic phase forms, the dispersion should appear optically transparent in the syringe barrel. Thus, the markings on the syringe barrel should be clearly legible through the mesophase in the barrel. In the case of colored proteins, the mesophase will have the color of the protein but will be optically transparent. Very slight cooling of the sample during mixing by placing the syringe mixer for a short time on ice, in a refrigerator or in the air stream of an air-conditioning unit can accelerate homogenization and the achievement of transparency. However, it is important not to overcool the sample, which can destabilize the cubic mesophase (**Fig. 1**), leading to protein damage.

**▲ CRITICAL STEP** Care should be taken to avoid extremely vigorous mixing, as this can cause sample temperature to rise due to frictional heating<sup>33</sup>. Although membrane proteins are usually more stable when reconstituted into a lipid bilayer, as is proposed to happen in the mixing process, high temperatures are not most likely to be good for the protein. Mixing comes

## PROTOCOL

about as a result of shear that develops as the material moves back and forth through the coupler. It is not known how shear will affect the protein, but it is expected that the gentler the mixing and the less shear imposed the better. Accordingly, we recommend that the rate of mixing should not exceed  $\sim 1$  stroke per s.

### ? TROUBLESHOOTING

**14|** To continue with the crystallization process, proceed directly to Step 15. Note that for the initial prescreening stage, the cubic phase and the conformation and activity of the protein reconstituted in the cubic phase may be evaluated as described in **Boxes 2** and **3**; when happy with the results of the analyses, fresh cubic phase should be prepared (Steps 1–13) before proceeding with Step 15.

### Setting up crystallization plates ● TIMING $\sim 10$ min per 27-well plate

**15|** At this juncture, the cubic mesophase has been formed and the protein is reconstituted into the lipid bilayer. The protein-loaded mesophase is now ready for dispensing into individual wells of the crystallization plates (Steps 29–33). First, however, the homogenous mesophase must be transferred to a 10- $\mu$ l Hamilton syringe (RN type) mounted on a repeating dispenser (**Fig. 8**). Begin this process by coupling the syringe to the repeating dispenser, as described in Steps 16–21 below. Then load the syringe, as described in Steps 22–28, with the cubic mesophase sample (prepared in Steps 1–13).

**16|** Remove the needle, but not the ferrule, from the 10- $\mu$ l syringe.

**17|** Remove the small flat retaining nut from the repeating dispenser with the aid of a small coin—a US cent works well. Be careful not to lose the rubber gasket on the syringe side of the retaining nut.

**18|** With the ratchet arm fully withdrawn, insert the syringe without its plunger through the holding ring of the dispenser.

**19|** Replace the retaining nut, gasket side facing the syringe, and screw it in tightly on the open end of the syringe.  
**▲ CRITICAL STEP** Care should be taken to ensure that the syringe is properly centered in the holding ring and that the barrel is aligned parallel to the ratchet arm. Both can be judged by eye. These two requirements are important because if the plunger does not run free and true or it is under strain due to bending or buckling at any point in its travel, pressure will build up in the source syringe during loading and catastrophic leakage can occur.

**20|** Pass the plunger through the gripping ring with the gripper nut unscrewed a few turns and guide the plunger into the open end of the syringe.

**21|** Depress the ratchet arm fully and move the plunger to the zero graduation mark on the barrel. The syringe is now ready for loading.

**22|** Move the plunger on one side of the assembled mixing unit (from Step 13) to the zero graduation mark to transfer the homogenous mesophase to the other syringe and the coupler.

**23|** Disconnect the empty syringe (with its ferrule in place) from the mixing unit and immediately connect the loaded syringe with the coupler attached to the threaded termination of the 10- $\mu$ l dispensing syringe.

**▲ CRITICAL STEP** The degree of tightness with which coupling is done is critical, as noted in Step 12. The degree of tightness can be gauged by feel, which benefits from practicing the coupling procedure.

**24|** Load the dispensing syringe by depressing the plunger in the 100- $\mu$ l syringe so that the mesophase transfers through the coupler. If coupling is tight and the plunger in the dispensing syringe runs free, then the plunger should begin to move in the direction of motion of the loading plunger as the dispensing syringe fills.

**▲ CRITICAL STEP** Care should be taken at this point to ensure that the loading plunger is not advanced to such an extent that the dispensing syringe fills to overflowing. This can happen suddenly with the plunger shooting out of the dispensing syringe. If this happens, all is not lost because the syringe is loaded and the plunger can simply be resealed. It can then be used in setting up a crystallization trial.

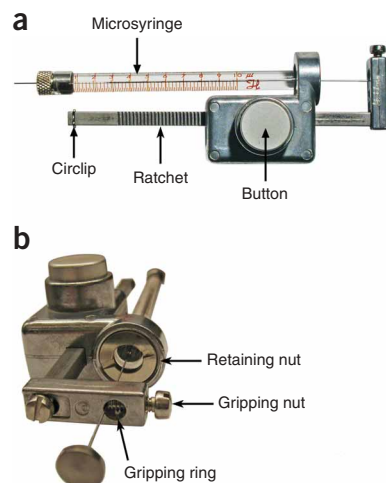


**Figure 8 |** Microsyringe-repeating dispenser. (a) Side view. (b) View from plunger end.

- 25| Disconnect the loading syringe with the coupler attached from the dispensing syringe.
- 26| Secure a short, flat-tipped needle to the steel termination of the dispensing syringe and carefully tighten it in place.
- 27| Clamp the plunger to the ratchet arm by tightening the nut in the gripping ring.  
**▲ CRITICAL STEP** Care should be taken not to overtighten the nut, as this can score and deform the plunger rendering it unusable.  
**▲ CRITICAL STEP** It is important that the travel range provided to the ratchet arm in the clamped condition be limited to no more than an inch (see **Fig. 8**). Beyond this, the plunger will have a tendency to buckle and delivery can fail.
- 28| Depress the ratchet drum several times to advance the plunger in the barrel, thereby filling the void volume of the needle and loading it. This step should be repeated (up to ten times) until a continuous string of the mesophase emerges from the tip of the needle. The syringe is now ready for use in setting up crystallization trials, which should commence immediately.  
**▲ CRITICAL STEP** It is not advisable to keep the protein-loaded cubic phase for too long before setting up the crystallization trials, as some proteins are unstable in the cubic phase without added precipitant.
- 29| Place the 27-well crystallization plate on a surface raised a few inches above the bench for ease of loading. Optimal contrast and enhanced visibility are achieved when the surface is black, or at least dark. Optionally, the outlet of a small ultrasonic humidifier can be directed toward the crystallization plate to slow evaporation from the dispensed bolus of mesophase during setup. This is especially relevant in areas where ambient relative humidity is low.
- 30| Homogenize the precipitant solutions, usually in a multiwell block, by shaking, centrifuge them at 3,000g and room temperature for 3–5 min (to consolidate solution and to pellet insoluble materials and dust particles) and place next to the crystallization plate for direct and easy access.
- 31| With the dispensing syringe held vertically in one hand, use the free hand to position the needle tip in the center and directly above the base of well no. 1. Press the button on the repeating dispenser to expel a bolus of mesophase onto the glass surface. The bolus volume is 200 or 100 nl when the standard repeating dispenser is used with a 10- or 5- $\mu$ l syringe, respectively.  
**▲ CRITICAL STEP** The tip of the needle should be no more than a few hundred micrometers above the base of the well to ensure proper delivery. If the tip is too far away, the mesophase will usually curl up and away from the base; if it is too close, the mesophase can ball up around the needle tip to be carried away stuck to the needle. Reproducible delivery is easily achieved. It just takes a little practice.
- 32| After the three wells in the first row on the plate are loaded with mesophase, place 1  $\mu$ l of precipitant solution on top of each mesophase bolus using a 2- $\mu$ l pipette and standard disposable tips.
- 33| Repeat Steps 31 and 32 two more times to fill three rows, each with three wells.
- 34| As quickly as possible, place a coverslip squarely over the nine filled wells to cover them uniformly.  
**▲ CRITICAL STEP** To effect a water-tight seal, use a wooden or a plastic spatula or rod to apply pressure to the coverslip where it makes contact with the exposed sticky surface of the spacer tape. Air gaps can be seen when present between the coverslip and the spacer surface. These can be eliminated by repeatedly working the spatula over the surface of the coverslip with moderate applied pressure. Avoid using anything harder than glass to apply pressure to the coverslip, as this may scratch the surface and impair well inspection for crystal growth.  
**▲ CRITICAL STEP** There are situations where it is necessary to open and reseal wells for purposes of soaking preformed crystals with heavy atoms or ligands, for example. In such cases, this is made possible by using 18 mm  $\times$  18 mm or 1 inch  $\times$  1 inch thick glass coverslips to cover anywhere from 1–4 wells. A thin layer of vacuum grease is applied to the exposed surface of the spacer ahead of loading. This renders the exposed surface nonsticky, but at the same time allows the well to be properly sealed when the coverslip is in place. The coverslip can be removed with relative ease and the well contents can be adjusted. The well can then be resealed with the original or a new coverslip. The process of opening and closing the well can be repeated as often as needed.
- 35| Repeat Steps 31–34 until all 27 wells are loaded and sealed. The plate is now ready for inspection and for incubation.

## ? TROUBLESHOOTING

### Incubation and tracking crystallogenesis ● TIMING 30–60 d

- 36| Place the plates in a temperature-controlled chamber, usually at 20 °C.  
**▲ CRITICAL STEP** It is possible to incubate the plates at other temperatures above and below 20 °C. It is important to note that below about 17 °C, the cubic phase of hydrated monoolein is no longer stable and can transform to the lamellar phase (**Fig. 1**), which is not compatible with *in meso* crystallogenesis. However, the cubic phase exhibits metastability and trials can be set up at lower temperatures, but this should be done with the knowledge that the system might convert to the lamellar phase at any

## PROTOCOL

time. Shorter-chained monoacylglycerols that work at such low temperatures have been designed, synthesized and purified, and one has been described in the literature<sup>35</sup>.

Light-sensitive proteins are usually handled by wrapping the plates in aluminum foil before placing them in the incubation chamber. These can be removed and examined under the microscope in subdued or appropriately colored light.

**37|** On a regular schedule, inspect the wells in crystallization plates using a PLM with a  $\times 10$  or  $\times 20$  objective. The schedule used in the authors' labs is as follows: day 0, 1, 2, 3, 5, 7, 14, 21, 30 and 60 post-setup. Carefully inspect the mesophase bolus adjusting the depth of focus within the 140- $\mu\text{m}$ -thick sample. Examination should be done both in normal light and between crossed-polarizers.

**▲ CRITICAL STEP** Some proteins produce crystals within a few hours; others can take months to grow. It is important to note that crystals can be short lived and can disappear. It is possible to miss them simply because the plates were not screened often enough. Thus, the frequency with which plates are screened is a judgment call. For those crystals that are slow to grow, the glass sandwich plates offer the advantage that they are essentially water-tight and do not dry out. We have measured this with 96-well plates and found them to undergo no measurable water loss over a period of at least 6 months in a temperature-controlled chamber at 20 °C (see ref. 28).

**▲ CRITICAL STEP** The cubic phase is optically isotropic and

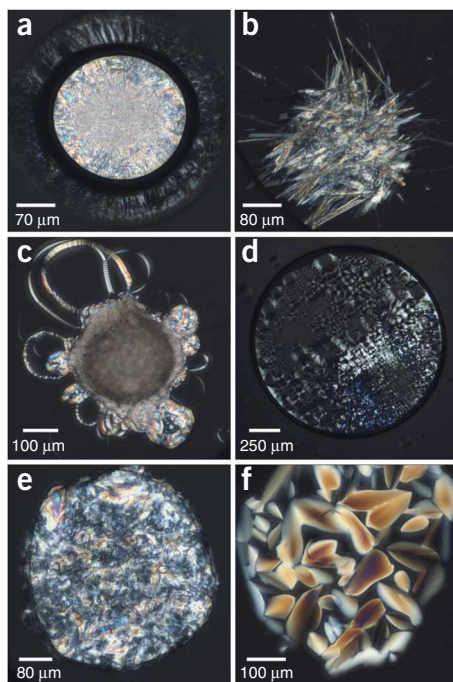


**Figure 10 |** Images of birefringent solid and liquid crystalline lipidic phases recorded using polarized light microscopy. (a) Dried-out lipid mesophase. This represents a typical outcome when the precipitant solution was either not dispensed or it dried out due to incomplete sealing. It most likely includes the L<sub>c</sub> and/or L<sub>α</sub> phases. (b) Crystalline L<sub>c</sub> phase. (c) L<sub>α</sub> phase. (d) Swollen L<sub>α</sub> phase. (e) Hexagonal phase. (f) Typical texture observed with a bolus incubated at pH > 9 that may have undergone hydrolysis and fatty acid production.

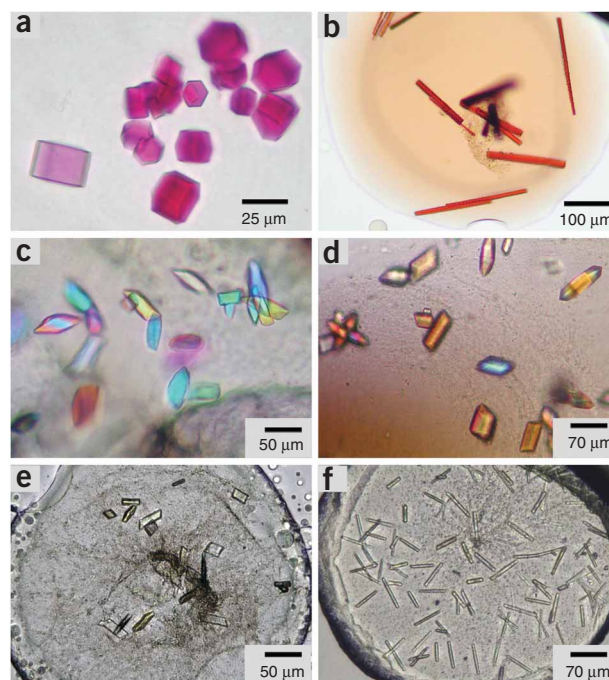


**Figure 9 |** Crystals of membrane proteins growing in the lipidic mesophase. (a) Bacteriorhodopsin; (b) light-harvesting complex II; (c) the adhesin/invasin OpcA; (d) the vitamin B<sub>12</sub> transporter, BtuB; (e) the engineered human  $\beta 2$  adrenergic receptor-T4 lysozyme chimera; (f) a carbohydrate transporter from *Pseudomonas*. All crystals were obtained by the authors.

when sandwiched between two glass plates, as in the case of the crystallization plates used here, optical quality is extremely good. This means that crystals of just a few micrometers in maximum dimension can be seen with ease using a standard light microscope (Fig. 9). The presence of crystals can usually be verified by viewing the bolus in the well between crossed polarizers. The cubic phase is not birefringent and appears dark just like the surrounding precipitant solution. In contrast, when nonisotropic crystals are present, they usually 'light up' and appear as sharp flecks of light in a dark background. Rotating the plate between the crossed polarizers can be used to pick out crystals in different orientations within the bolus.

**38|** Record the appearance of the mesophase taking care to note whether it is a stiff gel (characteristic of the cubic phase), is smooth and liquid-like (characteristic of the sponge phase) or is completely dissolved. Note too if it is birefringent or optically isotropic. If birefringent, its texture should be noted. Examples of images typically observed are included in Figure 10. Persistent birefringence associated with the lamellar or hexagonal phases suggests that the condition is unlikely to support growth of crystals.

**39|** Make a note of any crystal-like objects and of their appearance (shape, size, color, orientation and so on) and number. Carefully examine and note the birefringency of each. Nonbirefringent 'objects' with sharp edges can be voids in or single domains of the cubic phase (see Fig. 11). Initial hits

often appear as showers of tiny crystals most obvious when viewed between crossed polarizers. Tryptophan-containing protein crystals can be distinguished from salt, lipid or detergent crystals by imaging with a UV-fluorescence microscope in epi-illumination mode. Excitation and emission wavelengths should range from 280 to 300 nm and 340 to 400 nm, respectively (Korima microscope, **Fig. 12**). Absorption imaging at 280 nm is also possible<sup>36</sup> and/or the crystals can be harvested and examined for characteristic X-ray diffraction. Another option is to set up control crystallization trials using protein-free buffer.

**▲ CRITICAL STEP** To carry out UV-fluorescence imaging, it is necessary to use either quartz or UV-transmitting glass for the crystallization plate. The 0.5- to 1-mm-thick electroverre glass plates from Erie Scientific are suitable for this application.

**40|** Carefully examine any precipitated protein, if observed, in the mesophase. Birefringent precipitate may provide a useful initial condition for subsequent optimization. It is also possible that on further incubation the protein in the precipitate will convert to a crystal by Ostwald ripening<sup>37</sup>.

**41|** If desired, score the drops using a scoring system of the type included in **Figure 13** and log the data into a database for subsequent analysis of crystallization trials.

**Optimization ● TIMING 1–6 months**

**42|** When a crystallization hit has been recorded, initiate optimization to improve the size and/or diffraction quality. Strategies and protocols for performing optimization that are suitable for use in the *in meso* method have been described<sup>38</sup>. Also refer to **Box 5** for further information.

**Preparing to harvest crystals: opening the glass coverslip on a crystallization well in a glass sandwich plate**

**● TIMING 5–10 min**

**43|** If required, set up an ultrasonic humidifier near the microscope to increase local humidity and to minimize evaporation from the open drop during harvesting.

**44|** Place the plate on a bench and use the glass-cutting stone to score four lines in the form of a square into the coverslip. The square should be included within the dimensions of the crystallization well and be centered on the mesophase bolus.

**▲ CRITICAL STEP** None of the square should extend beyond the well onto the spacer. If it does, the coverslip cannot be removed intact because part of it will remain stuck to the spacer.

**▲ CRITICAL STEP** The glass sandwich crystallization plates are extremely useful for screening conditions that support crystallization. However, they are not particularly easy to harvest from. It is possible to set up *in meso* crystallization trials in plates from which harvesting is more facile, but the conditions for crystallization may not be the same and the new plates will usually require additional screening and optimization. In some cases, it is simplest to harvest directly from the glass plates. Harvesting from commercial plates is usually no different from

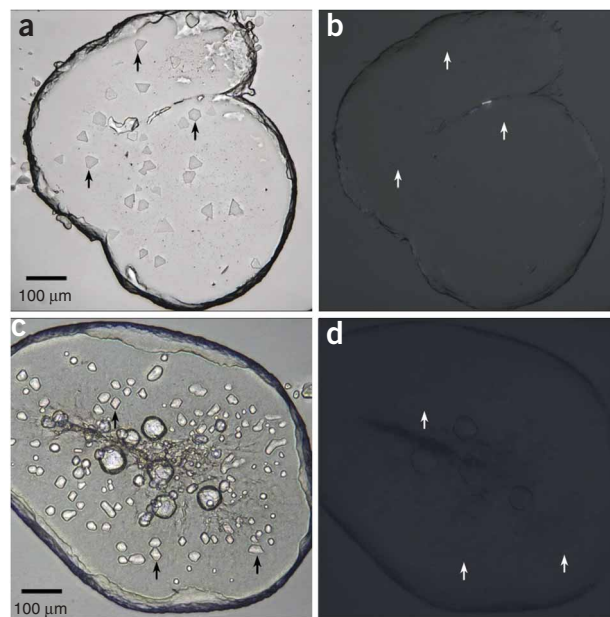
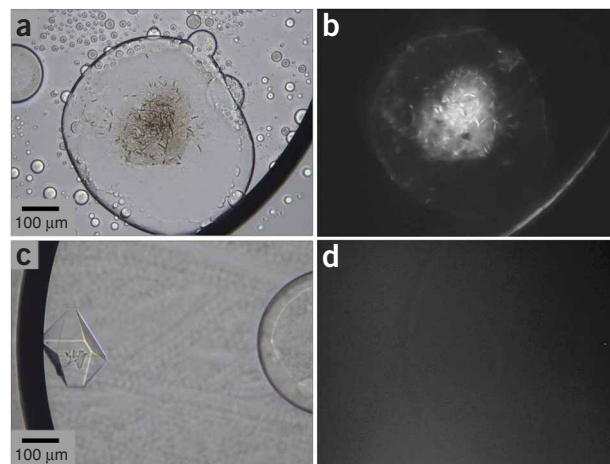


**Figure 11 |** Nonbirefringent ‘objects’ with sharp edges and corners that appear in lipid mesophases under *in meso* crystallization conditions. **a** and **c** are images observed with normal light. The corresponding images recorded between cross polarizers are shown in **b** and **d**. The angular objects most likely include domains of cubic phase, voids and trapped bubbles or droplets. Arrowed objects are for cross-referencing between images recorded with and without polarized light.

**Figure 12 |** Distinguishing protein from salt crystals. UV-fluorescence microscopy is shown here distinguishing (**a,b**) protein from (**c,d**) salt crystals growing in *in meso* glass sandwich plates. The protein is the engineered human  $\beta_2$  adrenergic receptor-T4 lysozyme chimera and the salt is sodium sulfate. Images in **a** and **c** were recorded with normal light. Images in **b** and **d** were recorded using a Korima fluorescence microscope with excitation and emission wavelengths of 280 nm (bandpass 20 nm) and 360 nm (bandpass 40 nm), respectively. Images were recorded with plates oriented ‘upside down’ such that the glass baseplate faces the incident exciting light source and the detector. Fluorescent protein crystals and precipitate can be seen in **b**. The salt crystal is not fluorescent and is not visible in **d**.

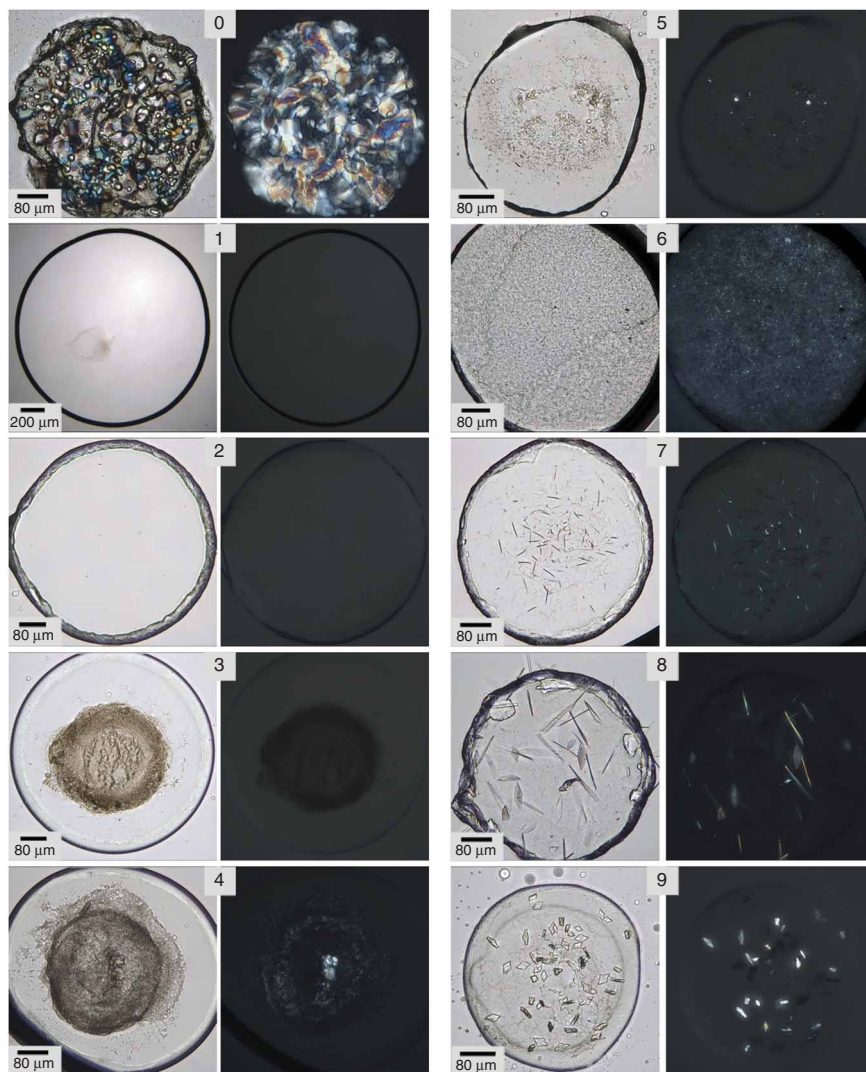




## PROTOCOL

**Figure 13** | A key for scoring the outcome of *in meso* crystallization trials. The scale runs from 0 to 9 and the corresponding images recorded in normal light (left panel) and between crossed polarizers (right panel) are shown.

0, birefringent mesophase. Certain precipitant solutions can trigger a conversion from the cubic to a lamellar or hexagonal phase, both of which are highly birefringent under cross-polarizers. Such mesophases are unlikely to support growth of protein crystals; 1, dissolved lipid. Some precipitants, such as MPD, PPO, Jeffamine M-600 and other organics, at high concentrations can dissolve the lipidic mesophase. This can often lead to the protein itself precipitating; 2, clear cubic phase. The cubic phase can be identified readily as being nonbirefringent, transparent and gel-like with rough edges; 3, precipitate. Here the protein forms a brownish, nonbirefringent precipitate. This often happens in the swollen cubic phase, the sponge phase or when the lipid completely dissolves. Drops with heavy precipitate are unlikely to yield crystals. Light precipitate can indicate that the condition is close to crystal nucleation. Often, crystals nucleate and grow in a drop with light precipitate; 4, birefringent precipitate. The protein precipitate has some birefringency under cross-polarizers. Optimization of this condition is recommended; 5, crystallites or spherulites. Protein forms birefringent particles that lack angularity or a well-defined crystal shape. This result can serve as a lead for optimization; 6, microcrystals. Crystals smaller than a few microns. Usually extensively nucleated producing 'showers' of birefringent dots most apparent when viewed under cross-polarizers; 7, needles. Crystals grow preferentially in 1 dimension. Size in the other two dimensions is at or below the resolving power of the microscope; 8, 2D plates. Crystals grow in two dimensions. Plate thickness is below the resolving power of the microscope; 9, 3D crystal. Crystals grow in three dimensions and all are clearly seen with a light microscope.



harvesting from glass sandwich plates, as described in Steps 52–55. Using plates made of low-birefringency plastic will greatly facilitate the process.

**45** | Place the scored well into viewing position on the stage of a stereomicroscope. Use low magnification, e.g.,  $\times 20$ , so that the whole well is in view.

**46** | With the tip of the tweezers, press on the glass outside and to one side of the square to fracture fully along the score line in the coverslip. Repeat this process along the other three sides.

**47** | Punch holes in the glass coverslip at diagonal corners, just outside the scored perimeter, using the fine tip tweezers.

**48** | Using a pipette, inject 2–3  $\mu\text{l}$  precipitant solution through one of the holes in the coverslip into the crystallization well to saturate the system with precipitant and to reduce the consequences of any dehydration that might occur.

**49** | Use the angled probe to free the square piece of glass from the rest of the coverslip.

**50** | Lift the freed glass square with the angled probe away from the well.

**▲ CRITICAL STEP** Carefully note the location of the mesophase, which can move while lifting the square cover. In most cases, the mesophase remains on the bottom of the well. Sometimes, however, it sticks to the upper glass coverslip. In this case, rotate the

freed square of glass and position it so that it rests on the plate next to the open well with its well side exposed. The angled probe can be used for this procedure.

### ? TROUBLESHOOTING

51| Immediately, add 2–5  $\mu\text{l}$  of precipitant solution to the exposed mesophase in the open well and/or on the upturned coverslip.

### Harvesting crystals ● TIMING 5–20 min

52| Increase the microscope magnification to  $\times 60$ – $100$ . Rotate the polarizer so that the crystal appears as a bright object on a darker background. Be careful to allow for sufficient light transmittance (in other words, do not fully cross the polarizing lenses) so that the loop remains visible while the mesophase and the crystal are manipulated.

### ? TROUBLESHOOTING

53| Use a Micromount of appropriate size to fish out a crystal.

▲ **CRITICAL STEP** Try to take as little mesophase with the crystal as possible. When the crystal resides deep inside the bolus, remove the overlaying mesophase to expose the crystal and to bring it to the surface using one Micromount and then harvest the crystal using a second, clean Micromount. A magnetic wand is used to facilitate handling the Micromount on its magnetic base.

▲ **CRITICAL STEP** It is also possible to free a crystal from the mesophase for harvesting by using enzymatic lipid hydrolysis<sup>39</sup>, detergent solutions<sup>40</sup> or mineral oils. However, these assorted manipulations can damage the crystal and lead to poor diffraction quality. In our hands, harvesting directly from the mesophase proved most successful with sensitive crystals and is recommended. Every effort should be made to minimize the amount of mesophase carried over with the crystal to reduce background scatter during diffraction data collection and to facilitate effective cryocooling.

54| Harvest the crystal and immediately and rapidly plunge it into clean (water-free) liquid nitrogen (LN<sub>2</sub>). Allow the Micromount, base and wand tip to cool to LN<sub>2</sub> temperature and then transfer the cryocooled sample into a precooled vial or a storage puck for storage and shipping.

▲ **CRITICAL STEP** The mesophase surrounding the crystal typically preserves the crystal during cryocooling. However, in rare cases, an additional cryoprotectant may be required. Considerations for the choice of the cryoprotectant are similar to those that apply to the cryocooling of soluble protein crystals and for membrane protein crystals prepared using more traditional *in situ* methods<sup>41</sup>. Typically glycerol, ethylene glycol, low molecular weight polymers, some organics and light mineral oils work well.

55| Record in a laboratory notebook the crystal identity, loop type and label, puck number and the location of the crystal in the puck. Add comments regarding crystal size, shape, color, location and orientation in the loop, as well as other useful information, such as the amount of mesophase carried over with the crystal.

### ● TIMING

Having assembled all the necessary tools, supplies and materials, it is possible to prepare the protein/lipid mesophase and to set up a single 27-well crystallization plate in about 30 min. With enough mesophase at hand, a second plate can be set up in another 10 min. These time durations apply to the dextrous novice and the experienced worker alike. Actual crystal-growing trials can extend from as short a period as a day all the way to months. Once usable crystals ( $\geq 25 \mu\text{m}$  in maximum dimension) are identified, harvesting and cryocooling can be done in 5–20 min. However, with some frequency, we encounter difficult samples where harvesting a single useful crystal can take an hour. And this was in the hands of an experienced worker. Usually what happens is that experience gained with difficult samples translates into substantially reduced harvesting times as the researcher becomes familiar with the rheology of the mesophase and with the response of the bolus and the crystal to the added precipitant, probing tools and harvesting loops.

Optimization on the basis of initial hits can produce crystals of diffraction quality within a single round of optimization that can take as little as a week. More usually, however, a series of optimizations is needed where aspects of the protein, the lipid, the precipitant, additives, bolus size, temperature and time are varied systematically. These rounds of optimization can take months to complete, but unfortunately there is no guarantee of success.

Establishing that a given ‘hit’ arises from the protein, as opposed to some other ingredient in the crystallization well, can be done simultaneously with imaging or viewing with a microscope if the protein is colored. If the protein contains tryptophan and a UV absorption or fluorescence microscope is available, the evaluation can be done in a matter of minutes. Longer time durations are needed to run protein-free controls and to make definitive diffraction measurements.

In preparation for setting up crystallization trials, glass sandwich plates must be silanized, perforated spacers applied and precipitant solutions chosen or formulated as needed. It is preferred to silanize plates and to apply spacers the morning or the day before a trial is to be set up. The time required depends on the number of plates involved. If preformulated precipitant solutions are to be used, it is simply a matter of selection. At the stage of optimization, precipitant solutions are usually

formulated by hand, using a multichannel pipette. The time required depends on the number of conditions to be screened and the number of ingredients in each. Typically, one 96-condition screen can be set up in an hour.

When trials are to be performed with mixtures of lipids, the corresponding samples should be prepared the previous day. This provides for overnight drying under high vacuum to ensure the lipid is solvent free at the point of use.

Mesophase, lipid and protein characterization, as part of quality control and gaining familiarity with the system under investigation, is desirable but not essential to perform crystallogenesis trials. Typically, such measurements are performed in parallel with ongoing trials. With all of the instrumentation and materials on site, it should be possible to make all of the thin-layer chromatography, PLM and small-angle X-ray scattering (SAXS) measurements in a single working day. Absorption, fluorescence and CD spectroscopies can also be completed in a day by an experienced researcher, with the proper equipment and materials at hand.

## ? TROUBLESHOOTING

### Step 13

#### Problem 1: cloudy mesophase

*Possible reason 1: Excess protein solution*

*Solution:* Occasionally, an excess of protein solution is used in which case a two-phase system results (see **Fig. 1**). This will give rise to a cloudy dispersion that will not clarify regardless of how much mixing is used. Although it is desirable to start out with a one-phase system in the interests of reproducibility, a slight excess of protein solution and a cloudy dispersion should not mean that the crystallization trial is to be abandoned, especially when working with a valuable protein and/or lipid. If a clear mesophase is required in such a situation, it can be obtained by supplementing the mixture with a small amount (typically <10% of the total mixture) of additional lipid. To this end, the homogenized sample should be moved to one of the syringes of the mixing unit, the empty syringe disconnected from the coupler and pure lipid added to it. The system is then reassembled, taking care to avoid trapping air bubbles. The overall composition should be mixed to restore the pure cubic phase, which is optically transparent.

*Possible reason 2: Excess lipid*

*Solution:* Cloudiness in the sample can also originate from inaccurate weighing of the lipid and/or protein solution, or from leaks in the syringe. The consequence here is that the system is less hydrated than is required for cubic-phase stability. If this causes the lamellar phase to form or for the lamellar and cubic phases to coexist (see **Fig. 1**), cloudiness can result. A check on this can be made by transferring all of the homogenized mesophase from one of the syringes and recording total mesophase volume in the other. The value should match closely the sum of the starting lipid and protein solution volumes taking account of the coupler dead volume, which is typically 1.5  $\mu\text{l}$  (see ref. 33). If the recorded volume is considerably less than expected and the dispersion is cloudy, it is important to check the system for leaks and to repeat the mixing protocol with nonleaking syringes.

*Possible reason 3: Trapped air*

*Solution:* Trapping air and bubbles in the lipid and/or protein solution and at the stage where the syringes are combined with the coupler will also give rise to cloudiness and should be avoided if at all possible. Again, this is done in the interests of uniformity and reproducibility.

*Possible reason 4: High concentration of detergent in the protein solution*

*Solution:* A high concentration of detergent in the protein solution can destabilize the cubic phase and transform it fully or partially into a lamellar phase<sup>32</sup>. This is usually accompanied by the formation of a cloudy dispersion that does not clear with mixing. The problem can be diagnosed by examining the phase texture of a few hundred nanoliters of the dispersion by polarized light microscopy (see **Box 2**). If the lamellar phase is confirmed, the protein can be treated to reduce detergent carryover. This might involve reducing the detergent concentration in the buffer used to elute the protein from a column by washing with a lower detergent concentration buffer at the concentration step, by using higher molecular weight cutoff filters during concentration and/or by using detergent-binding materials, such as Bio-Beads SM-2. It is still possible to perform successful *in meso* crystallization trials starting from predominately lamellar phase because certain precipitants, highly concentrated salt solutions in particular, can cause the system to revert to the cubic phase (see ref. 32, for an example).

#### Problem 2: leakage at the coupler

*Possible reason: Loose connection*

*Solution:* Torque should be maintained during the mixing process by applying a small but steady clockwise, rotating force to the two syringes on either side of the coupler. This is to minimize the likelihood of leakage. We have found that leaks are less of a problem when a tight wrap of Parafilm is applied to the coupler that extends up the base of the two syringes. The 'bandaging' is done within about 20 or so strokes when mixing is known to be progressing properly.

#### Problem 3: syringe leakage

*Possible reason 1: Broken syringe*

*Solution:* Excessive force applied to the plunger in the barrel of a Hamilton syringe can cause the glass barrel to break or to leak at the junction between the barrel and the threaded steel barrel termination. Syringes that have failed in this way should be discarded.

*Possible reason 2:* Worn-out Teflon plunger tip

*Solution:* The Teflon tip at the top of the plunger can wear out from overuse and may start leaking. Replacement plungers for gas-tight syringes are available through Hamilton and are interchangeable between syringes.

**Problem 4: difficulty with mixing**

*Possible reason:* Nonuniform mixing

*Solution:* When the lipid and the protein solution come into contact at the beginning of the mixing cycle, extra force may be needed to move the contents of the syringe through the coupler. This is to be expected, as different phases form depending on the degree of hydration (see **Fig. 1**). However, excessive force should not be used, as this will cause the glass barrel to break or the syringe to leak (see previous **? TROUBLESHOOTING** items). Instead, it is recommended that the mixing direction be reversed and that less than complete strokes be used to induce local homogenization. With time, the full mixing stroke can be implemented as the syringe contents become more uniform.

**Step 35**

**Problem: failure to dispense**

*Possible reason:* Clogged needle, coupler

*Solution:* It is important not to leave syringes loaded with mesophase open to the atmosphere for more than a few minutes. Otherwise, the mesophase can dry out and plug the exposed orifice of a needle, barrel termination or coupler. Although these can be cleaned and recovered for reuse, it usually involves considerable effort and time. Accordingly, it is best to use the material as quickly as possible and then to dismantle the device and to thoroughly wash the syringes, needles, couplers, ferrules and so on with methanol followed by milli-Q water and then to dry everything in a stream of compressed dry air or nitrogen gas.

**Step 50**

**Problem: nonviscous mesophase**

*Possible reason:* Formation of the less viscous sponge phase

*Solution:* The sponge phase is a variant of the cubic phase that forms in the presence of certain precipitants<sup>22</sup>. Depending on the protein, harvesting small crystals from the sponge phase can be more difficult than those from the cubic phase. The former is much less viscous and can flow. Thus, when the glass coverslip square is broken to access the well, capillarity draws the sponge phase and its crystal cargo to the edge of the square where it typically mixes with shards of glass. Although the shards are not birefringent and can usually be distinguished from protein crystals, their presence complicates harvesting. Further, the sponge phase is 'stringy' and excess sponge phase can get carried along with the crystal on the Micromount during harvesting. To overcome these problems, a small amount of modified precipitant solution is added to the well as soon as it is opened to regenerate the original, viscous cubic phase. This is achieved by using a lower concentration of sponge-inducing agent in the precipitant solution than was used during the original trial. The conversion takes several minutes at which point harvesting from the cubic phase can proceed as described above. The one risk associated with this solution is that the transformation back to the cubic phase can destroy the crystal, which formed under conditions that gave rise to the sponge phase. But in our hands, and especially when working with crystals of GPCR, this approach generally increases the yield of successfully harvested crystals compared with working with the sponge phase directly.

**Step 52**

**Problem: crystals are not visible under cross-polarized light**

*Possible reason:* Isotropic space group, orientation issue

*Solution:* The ability of the crystal to rotate polarized light, and thus its birefringence and visibility, depends in part on the crystal space group and on the orientation of the crystal with respect to the polarizing filters. Sometimes the crystallization plate or the crystal itself must be rotated in the light beam of the microscope to increase or restore crystal birefringency.

**Box 2**

**Problem: dehydration**

*Possible reason:* Sample exposed to atmosphere for too long

*Solution 1:* If the mesophase dries out, even slightly (see phase diagram, **Fig. 1**), it can transform to another phase. The chances of this happening can be reduced by performing Step (ii) of Section B, Polarized Light Microscopy, in **Box 2** as fast as possible and in a humid atmosphere. Use of a humidifier close to where the work is being done is recommended if problems with drying are encountered. It is also possible to raise local humidity by placing water-saturated tissues in a circle around the microscope slide. Alternatively, the mesophase can be covered with bathing solution as soon as it is placed on the slide and then capped



with a coverslip as above. In this case, the bathing solution, which is isotropic, will appear dark when viewed between crossed polarizers. The choice of bathing solution will depend on the composition of the original sample. If it was prepared with protein solution, the corresponding protein-free and detergent-free buffer is appropriate. This can be verified by monitoring the PLM texture of the mesophase bolus, which should not change with time.

**Solution 2:** One must also be careful that the system does not lose an excessive amount of water, in which case it can transform to the fluid isotropic liquid. The fluid isotropic liquid is nonbirefringent similar to the cubic phase and if it is accessed, it can lead to a case of mistaken phase identity. However, a fluid isotropic bolus can be distinguished by its edges that are uniform and usually circular, reflecting the fact that it is a liquid. In contrast, a cubic phase bolus is stiff with edges that appear angular and retain a defined shape.

**Box 3**

**Problem: high UV absorbance**

**Possible reason:** Presence of trace impurities in the lipid

**Solution:** Despite the fact that the lipid used can be >99% pure, as judged by thin-layer chromatography and NMR, the UV absorbance of the mesophase can be considerable<sup>42</sup>. This problem of ‘background’ absorbance is exacerbated because the cubic phase sample is close to 60% (wt/wt) or 1–2 M lipid. Thus, a small amount of a highly absorbing contaminant in the lipid will contribute significantly to the background signal. Effort has been made to find commercial and homemade lipid with lower absorbance, but to no avail. The precise origin of the absorbance signal is not known. Thus, to quantify the spectral properties of the reconstituted protein, all spectra are recorded against an air reference. The analyte protein spectrum is obtained by subtracting the lipid/buffer background from the protein/lipid/buffer sample spectrum.

**ANTICIPATED RESULTS**

Four examples of membrane protein crystallizations by the *in meso* method that have led to high-resolution structures are presented below.

**The vitamin B<sub>12</sub> transporter, BtuB: a well-behaved and robust membrane protein**

BtuB is an outer membrane protein from the TonB-dependent transporter family responsible for the uptake of cyanocobalamin (Vitamin B<sub>12</sub>) in gram-negative bacteria. The protein was overexpressed in *E. coli* and purified as described<sup>43</sup> using 1.5% (wt/vol) octylglucoside and 0.1% (wt/vol) LDAO (N-Lauryl-N,N-dimethylamine oxide) during extraction and purification, respectively. Purified protein was concentrated to 10–15 mg ml<sup>-1</sup> in 10 mM Tris (pH 8.0), 0.1 M NaCl and 0.1% (wt/vol) LDAO.

Mixing the protein solution with monoolein in a 2:3 weight ratio yielded the cubic-Pn3m phase as evidenced by SAXS (Fig. 14; refer to Fig. 15 for typical SAXS patterns from the different mesophases most likely to be encountered while working with hydrated lipids). A variety of spectroscopies were used to characterize the protein reconstituted in the lipidic mesophase. These were made possible using an assortment of microcuvettes and accessories (Fig. 16) as described in Box 3. The protein was inserted into the bilayer of the cubic phase, which was verified using tryptophan fluorescence quenching by a brominated monoacylglycerol (Fig. 17). The secondary structure of the reconstituted protein was undistinguishable from that of the protein in detergent solution as judged by circular dichroism measurements (Fig. 17). Finally, the ability of the *in meso* reconstituted protein to bind vitamin B<sub>12</sub> with native-like affinity was shown by *in situ* binding measurements<sup>23</sup> (Fig. 17).

*In meso* crystallization was performed with monoolein as the host lipid. The lipidic mesophase laden with protein was dispensed into homemade 96-well glass sandwich crystallization plates using a home-built *in meso* crystallization robot. Trials were performed with 50 nl of protein–lipid dispersion and 1 µl of precipitant solution. Plates were incubated at 20 °C for up to 30 d. Crystallization was monitored using an automatic imager (RockImager RI54) and manually by light microscope. Initial

**Figure 14 |** Small-angle X-ray diffraction patterns of hydrated monoolein in the cubic and sponge phases. Samples were prepared with (a) water, (b) apo-BtuB protein solution and (c) apo-BtuB protein solution followed by incubation with MPD-containing precipitant for 16 d at 20 °C. The cubic-Pn3m phase with lattice parameters of 104.8 and 104.3 Å was recorded in a and b, respectively. The diffuse ring surrounding the beam stop shadow in c is characteristic of the L3 or sponge phase. Samples were prepared with 60% (wt/wt) monoolein and 40% (wt/wt) water in a, 60% (wt/wt) monoolein and 40% (wt/wt) protein solution (12.9 mg BtuB/ml in 20 mM Tris-HCl (pH 8.0), 0.1 M NaCl, 0.1% (wt/vol) LDAO in b and c. In c, 2 µl of the lipid/protein mesophase in an X-ray capillary tube was overlain with 10 µl of precipitant solution containing 10% (vol/vol) MPD, 0.2 M ammonium formate, 50 mM MES (pH 6.5) and incubated for 16 d at 20 °C before data collection. Microcrystals of BtuB were present in c at the end of the incubation period. Reproduced with permission from ref. 23.

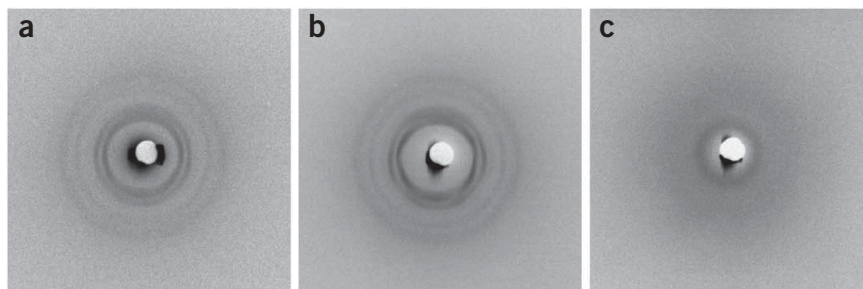
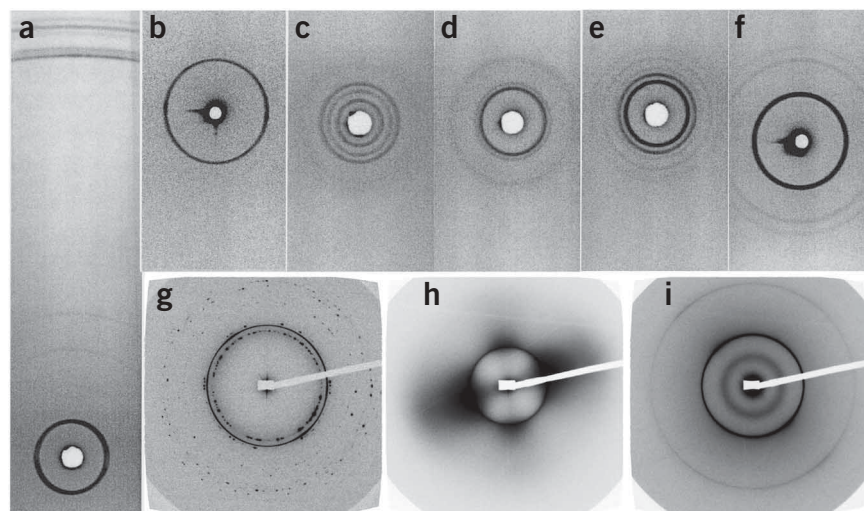


**Figure 15** | X-ray diffraction patterns of the various phases that can occur in the monoolein/screen solution/water system. Phase identity follows: (a) Lc phase. (b)  $L_{\alpha}$  phase. (c) Cubic-Im3m phase. (d) Cubic-Ia3d phase. (e) Cubic-Pn3m phase. (f)  $H_{II}$  phase. (g)  $L_{\alpha}$  and cubic-Ia3d phase coexistence. The cubic phase pattern is spotty because of the presence in the sample of relatively large monodomains (see ref. 47). (h)  $L_{\alpha}$  phase in conjunction with extensive diffuse scattering. (i)  $L_{\alpha}$  phase and disordered cubic (inner diffuse ring) phase coexistence. Diffraction images are from ref. 48. Bragg reflection indices are detailed in ref. 49.



screening was performed using six 96-well blocks filled with precipitant solution from commercial crystallization kits (Crystal Screen HT, Index HT, SaltRx and MembFac from Hampton Research; Wizard I&II from Emerald BioSystems; MemStart from Molecular Dimensions and JBScreen Membrane from Jena Bioscience). Small crystals of the type shown in **Figure 18** were found to be formed in the presence of MPD (2-methyl-2,4-pentanediol), pentaerythritol propoxylate (5/4 PO/OH), PEG 550 MME, jeffamine M-600, 1,4-butanediol and potassium thiocyanate. Conditions containing MPD were optimized using coarse concentration  $\times$  pH grid screens ([MPD] range 6–14% (vol/vol) with 2% (vol/vol) steps, pH range 4–8 with 1 pH unit steps), followed by screening with 48 different salts as additives (two concentrations for each salt in the 0.1–0.5 M range) and finishing with fine concentration  $\times$  pH grid screens ([MPD] range 8–12% (vol/vol) in steps of 1% (vol/vol), salt concentration range 0.05–0.3 M in 0.05 M steps, pH range 6–7 in pH unit steps of 0.5). About five subsequent rounds of optimization (using visual, not diffraction quality cues) were needed to obtain  $\sim 100\text{-}\mu\text{m}$ -sized BtuB crystals. The best crystals were grown in 10–12% (vol/vol) MPD, 0.1–0.2 M ammonium formate and 0.1 M MES (pH 6.5). Crystals of BtuB for crystallographic measurement were grown in a 72-well Nunc microbatch plate using a fine concentration  $\times$  pH grid screen around the best conditions found with sandwich plates. A quantity of 200 nl of lipid–protein dispersion was used in each well in conjunction with 3  $\mu\text{l}$  of precipitant solution. Wells were sealed with transparent tape. Crystals grew to their full size ( $\sim 100\text{ }\mu\text{m} \times 60\text{ }\mu\text{m} \times 25\text{ }\mu\text{m}$ ) in 10–14 d (**Fig. 9d**). Harvesting was done after 14 d using Hampton cryoloops (0.1 mm diameter) and crystals were cryocooled and stored in liquid nitrogen. Lipidic cubic phase that had swollen in the presence of MPD and that had transformed into a sponge phase had the consistency of a viscous liquid, which did not interfere with harvesting. MPD and lipid served as cryoprotectants and no additional cryoprotectant was used.

Diffraction data from several crystals were collected on the F1 beamline at the Cornell High-Energy Synchrotron Source (CHESS). Best sets from two different crystals were merged to obtain complete data at 1.95 Å.

### Light-harvesting complex II: working with a chromophore-containing protein and short-lived crystals

Light-harvesting complex 2 (LH2) functions as an antenna to trap light energy and to pass it to the reaction center in photosynthetic bacteria. Wild-type LH2 was purified using 0.05% (wt/vol) LDAO from *R. acidophila* as described<sup>44</sup> and was concentrated to 20–30 mg ml<sup>-1</sup> in 20 mM Tris (pH 8.0), 0.05% (wt/vol) LDAO.

Samples for use in crystallization trials were prepared with 60% (wt/wt) monoolein and 40% (wt/wt) protein solution (20–30 mg protein per ml) using the lipid-mixing device. The UV-visible absorption spectrum of LH2 reconstituted in the cubic phase was similar to that obtained with the protein in detergent solution with one difference; a slight distortion in the bacteriochlorophyll absorption bands was observed and

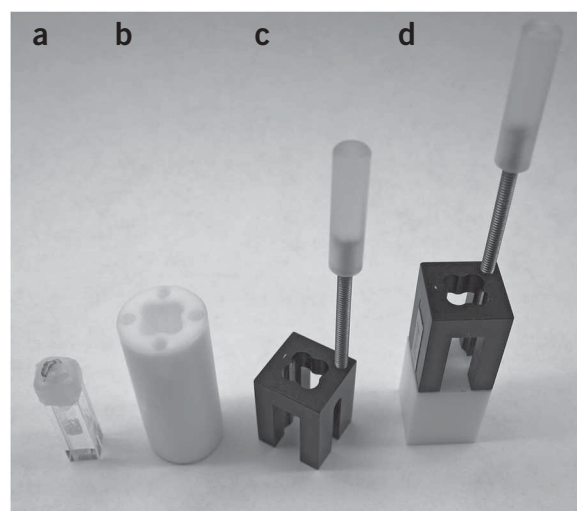
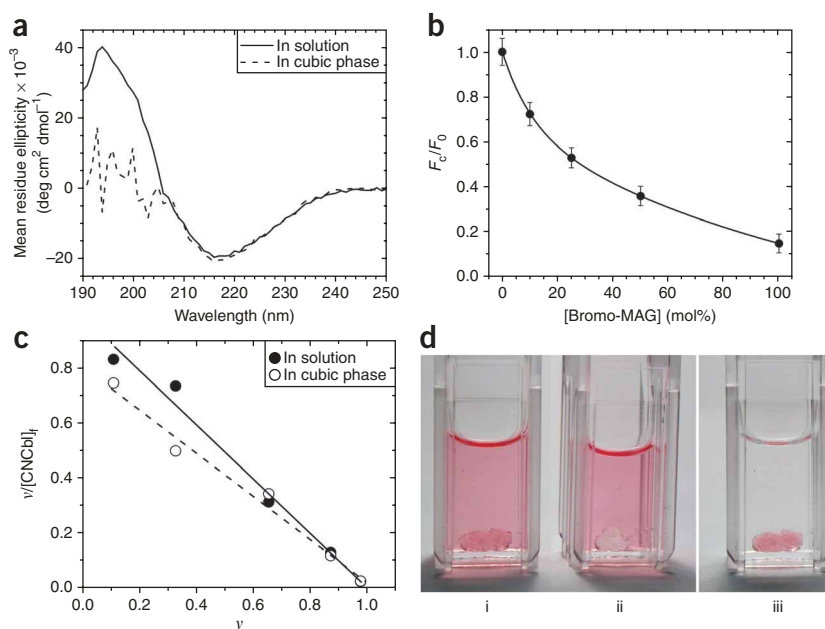


**Figure 16** | Spectrophotometry/fluorescence cuvette and accessories. (a) 3-mm pathlength cuvette containing optically clear lipidic cubic phase following centrifugation. (b) Teflon cuvette holder for centrifugation. The holder fits inside a 15-ml Falcon tube. (c) Adapter for 3-mm cuvette that fits into a standard (1 cm  $\times$  1 cm) spectrophotometer or fluorimeter cuvette holder. (d) The same adapter as in c resting on a Teflon shim to position the cuvette in the light beam of a Beckman spectrophotometer.

**Figure 17** | Spectrophotometric and visual properties of BtuB in detergent solution and in the cubic phase. **(a)** CD spectra of apo-BtuB in detergent solution and in the cubic phase. The region of the cubic phase spectrum below  $\sim 208$  nm is not reliable because of strong background absorption by the lipid, as described<sup>42</sup>. **(b)** Quenching of apo-BtuB intrinsic fluorescence by bromo-MAG in the cubic phase of hydrated monoolein. Fluorescence intensity ( $F_c$ ) was normalized to the value recorded in the absence of quenching lipid ( $F_0$ ). Values reported are the average of at least triplicate sample preparations. **(c)** Scatchard analysis for the binding of CNCbl to apo-BtuB in micellar solution (solid circles) and in the cubic phase of hydrated monoolein (open circles). The corresponding dissociation constant,  $K_d$ , values are 1.02 and 1.24 nM, respectively. **(d)** Photograph of a bolus of cubic phase (i, iii) with and (ii) without reconstituted apo-BtuB equilibrated for 6 d at 20 °C with a solution of 67  $\mu$ M CNCbl. In (iii), the bathing CNCbl solution was replaced with CNCbl-free buffer just before the photograph was taken to make the labeling of the bolus more obvious. The bolus of cubic phase can be seen as an elliptically shaped object at the bottom of a cuvette. Adapted from ref. 23.



attributed to constraints imposed on the protein by the bilayer curvature of the mesophase (**Fig. 19**). Initial crystallization screening was performed with the *in meso* robot. To this end, each well in a homemade, 96-well glass sandwich crystallization plate was loaded with 50 nl of lipid-protein dispersion followed by 1  $\mu$ l of precipitant solution at room temperature. Four commercial screens were performed in duplicate. Incubation was carried out in a temperature-regulated dark chamber at 20 °C. Crystallization progress was evaluated several times in a 2-week period using an automatic imager (RockImager RI54) and manually by microscope. Initial crystal hits were found in a number of conditions containing precipitants that cause the cubic phase to swell, such as MPD, pentaerythritol propoxylate (PPO), 1,4-butanediol and Jeffamine M-600. Optimized conditions leading to diffraction quality crystals included 20% (vol/vol) PPO, 0.1 M potassium acetate and 0.1 M Tris-HCl (pH 8.0) (see ref. 22). Crystals typically grew as long rods ( $\sim 200 \mu\text{m} \times 30 \mu\text{m} \times 10 \mu\text{m}$ ) for 3–7 d (**Fig. 9b**). After 7–10 d, the crystals began to degrade. Therefore, harvesting was carried out within a week of setup to ensure best crystal quality.

A full 2.45-Å data set was collected from a single crystal on the F1 beamline at CHESS.

### Adhesin, OpcA: use of inclusion bodies

OpcA is an integral outer membrane adhesin protein from *N. meningitidis*, the causative agent of meningococcal meningitis and septicemia. It binds to sialic acid-containing polysaccharides on the surface of epithelial cells. Recombinant OpcA was obtained by expression of the protein into inclusion bodies, followed by solubilization in guanidine HCl and rapid dilution into buffer containing LDAO<sup>45</sup>. Subsequent purification was carried out as described previously<sup>45</sup>. After the last purification step, the protein was precipitated in ethanol and stored in small aliquots at  $-20$  °C. Before crystallization, a vial of the protein-in-ethanol suspension was centrifuged for 15 min at 14,000g at 4 °C. Ethanol was removed and the pellet was dissolved in 0.1% (wt/vol) DDM (n-dodecyl- $\beta$ -D-maltopyranoside), 50 mM bis-tris propane (pH 7.0) to 0.2 mg of protein per ml. The protein was then concentrated using a Microcon spin concentrator with 30 kDa cutoff to 10–15 mg ml<sup>-1</sup>.

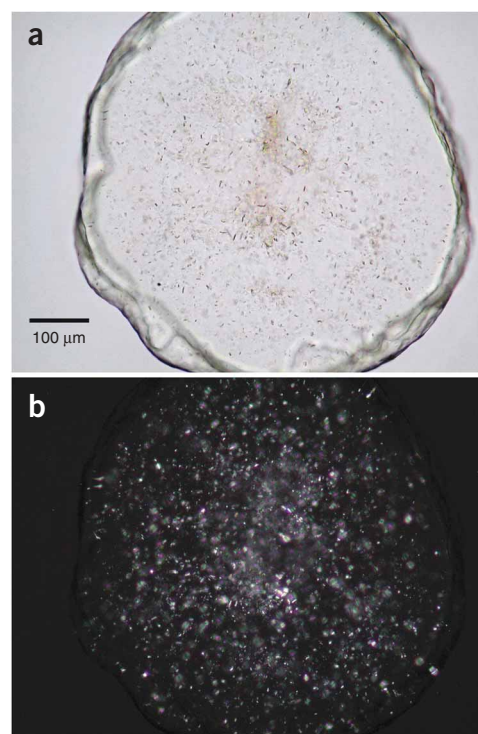


**Figure 18** | Initial BtuB microcrystal hits. Pictures were taken using **(a)** brightfield illumination and **(b)** using cross-polarizers on the fourth day after setup. Precipitant: 0.05 M magnesium chloride, 30% (vol/vol) PEG 550 MME, 0.1 M HEPES (pH 7.5).

*In meso* crystallization was performed with monoolein as the host lipid. The lipidic mesophase laden with protein was prepared as 3:2 volume mix of lipid and protein solution and dispensed into homemade 96-well crystallization plates using a home-built *in meso* crystallization robot. Trials were performed with 50 nl of protein–lipid dispersion and 1  $\mu$ l of precipitant solution. Plates were incubated at 20 °C for up to 30 d. Crystallization was monitored using an automatic imager (RockImager RI54) and manually by light microscope. Initial screening was performed using six 96-well blocks filled with precipitant solution from commercial crystallization kits (Crystal Screen HT, Index HT, SaltRx and MembFac from Hampton Research; Wizard I&II from Emerald BioSystems; MemStart from Molecular Dimensions and JBScreen Membrane from Jena Bioscience). Small crystals were found to be formed in the presence of PEG 400 and lithium sulfate. Initial conditions were optimized using concentration  $\times$  pH grid screens and different salts as additives to obtain  $\sim$ 70- $\mu$ m-sized crystals (Fig. 9c). The best crystals were grown in 18% (vol/vol) PEG 400, 0.1 M potassium sulfate, 0.05 M HEPES (pH 7.0) (see ref. 24).

Crystals of apo-OpcA for crystallographic measurement were grown in a 96-well Greiner sitting-drop plate. A total of 200 nl of lipid–protein dispersion was used in each well in conjunction with 2  $\mu$ l of precipitant solution. Each reservoir contained 50  $\mu$ l of the corresponding precipitant solution. Wells were sealed with transparent tape. Crystals grew to their full size (25  $\mu$ m  $\times$  25  $\mu$ m  $\times$  70  $\mu$ m) in 20–30 d. Harvesting was done after 24 d using Hampton cryoloops (0.05–0.1 mm diameter) and crystals were cryocooled and stored in liquid nitrogen. Crystals were harvested directly from the lipidic cubic phase and were frozen immediately without further treatment. During harvesting, care was taken to pick up as little mesophase as possible. PEG 400 and lipid served as cryoprotectants and no additional cryoprotectant was used.

A full data set at 1.95 Å was collected from a single crystal on the F1 beamline at CHESS.

### Engineered human $\beta_2$ -adrenergic receptor: working with a highly unstable protein, microcrystals and a lipid additive

The  $\beta_2$ -adrenergic receptor ( $\beta_2$ AR) is a member of the GPCR family. It regulates cardiovascular and pulmonary function in response to elevated levels of the endogenous hormones, adrenaline and noradrenaline. To increase its stability and aid in crystallization, the human  $\beta_2$ AR was modified as follows<sup>46</sup>:

- (i) The third intracellular loop was replaced with a compact and stable protein lysozyme from T4 phage,
- (ii) The C-terminal 48 amino acids were removed, and
- (iii) A glycosylation site at Asn187 was mutated to Glu.

The engineered protein, called  $\beta_2$ AR-T4L, was expressed in sf9 insect cells infected with baculovirus. The protein was solubilized in DDM and purified as described in ref. 46. Purified protein was treated with iodocetamide to block free sulfhydryls and additionally stabilized by a partial inverse agonist carazolol and concentrated to 30–50 mg ml<sup>-1</sup> for crystallization trials.

Initial crystallization screening in lipidic cubic phase was performed with glycosylated and deglycosylated (treated with PNGase F) receptors using monoolein as host lipid against seven commercial 96-well screen kits in duplicate. Trials were set up in 96-well glass sandwich plates using 50 nl of lipidic cubic phase and 0.8  $\mu$ l of precipitant solution per well dispensed by the *in meso* robot. Initial hits consisting of showers of microneedles (<5  $\mu$ m in length; Fig. 20) were obtained only with deglycosylated protein at three different conditions, all containing PEG 400, lithium sulfate and a buffer at pH between 6.5 and 8. Precipitant and salt concentration  $\times$  pH optimization

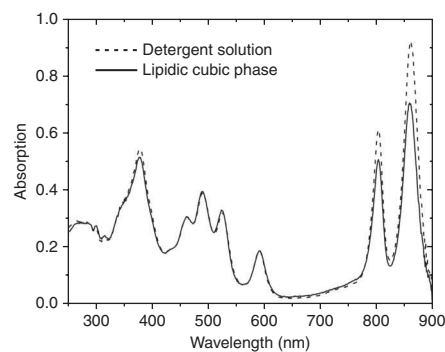


**Figure 19** | Absorption spectrum of LH2 in detergent solution and in the lipidic cubic phase. Spectra were recorded 15 min after protein dilution into detergent solution (dashed line; 0.035 mg ml<sup>-1</sup>) or reconstitution in the cubic phase (solid line; 50% (wt/wt) monoolein, 0.07 mg ml<sup>-1</sup>). Reproduced with permission from ref. 22.

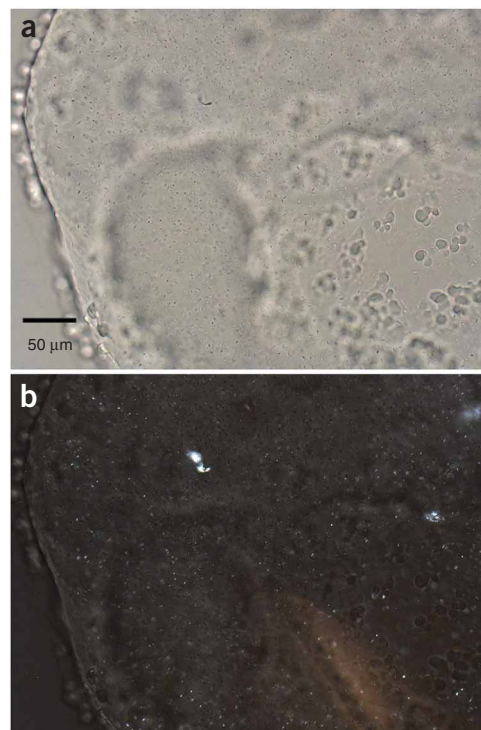


**Figure 20** | Initial  $\beta_2$ AR-T4L microcrystal hits. Pictures were taken using (a) brightfield illumination and (b) cross-polarizers on the third day after setup. Precipitant: 0.1 M lithium sulfate, 0.1 M sodium chloride, 30% (vol/vol) PEG 400, 0.1 M HEPES (pH 7.5).



grids combined with salt identity optimization provided useful ranges and optimal values for PEG 400 and salt (sodium sulfate was identified by screening for salt identity) concentrations and buffer pH, and yielded slightly larger crystals measuring 15  $\mu\text{m} \times 5 \mu\text{m} \times 1 \mu\text{m}$ . The most dramatic improvement came from screening with soluble and lipophilic additives. We have found that the addition of cholesterol to the host lipid and of 1,4-butanediol to the precipitant solution significantly improved the shape and size of crystals to an average of 30  $\mu\text{m} \times 10 \mu\text{m} \times 5 \mu\text{m}$ . Finally, the conditions were fine-tuned, as a result of which the buffer was changed from HEPES to Bis-tris propane, the lipidic cubic-phase bolus size was reduced from 50 to 20 nl and the protein concentration was increased from 30 to 50 mg ml<sup>-1</sup>. To arrive at the final crystallization conditions consisting of 30–35% (vol/vol) PEG 400, 0.1–0.2 M sodium sulfate, 0.1 M Bis-tris propane (pH 6.5–7.0) and 5–7% (vol/vol) 1,4-butanediol as the precipitant solution and 8–10% (wt/wt) cholesterol in monoolein as the host lipid, we formulated thirty-five 96-well screens and performed over 15,000 trials. Therefore, robotics were indispensable to achieve success in this project. The fully optimized crystals were grown for 3–6 d and reached a maximum size of 40  $\mu\text{m} \times 20 \mu\text{m} \times 7 \mu\text{m}$  (see ref. 25) (**Fig. 9e**).

Extensive attempts to reproduce crystals in commercial plates for microbatch, and for sitting and hanging-drop vapor diffusion, resulted in significantly smaller crystals. Therefore, crystals were harvested directly from the glass sandwich plates. Crystals were scooped from lipidic cubic or sponge phase using MiteGen 30 or 50  $\mu\text{m}$  MicroMounts and plunged into liquid nitrogen. Owing to difficulties of harvesting small crystals from sponge phase (see TROUBLESHOOTING advice for Step 53), the concentration of PEG 400 was lowered to ~26% (vol/vol) to transform the sponge phase into a cubic phase before harvesting. Care was taken to reduce the amount of mesophase that came with the crystal onto the mount so as to minimize unwanted background X-ray scattering. Attempts to dissolve the mesophase either by increasing the concentration of PEG 400 or by using mineral oils typically resulted in a reduction in the diffraction power of the crystals.

As the crystals were so small, it was necessary to use an equally small but highly collimated X-ray beam for diffraction data collection. Accordingly, data were collected using a 10- $\mu\text{m}$ -diameter minibeam on the 23 ID-B beam line (GM/CA CAT) at the Advanced Photon Source. Crystals diffracted better than 2.2- $\text{\AA}$  resolution but were susceptible to radiation damage. Therefore, a complete, low-resolution data set, collected with a highly attenuated beam, was merged with 31 high-resolution small sets of 10–20 degrees each to obtain complete data at 2.4- $\text{\AA}$  resolution<sup>25</sup>.

**ACKNOWLEDGMENTS** We thank members and associates of the Caffrey group, past and present, for their assorted contributions over the years to this work. In particular, we acknowledge the contributions of D. Aragao, A-c Cheng, J. Clogston, D. Hart, N. Hoefler, B. Hummel, D. Li, W. Liu, J. Lyons, Y. Misquitta, L. Muthusubramaniam, A. Peddi, B. Sun, J. Tan and Y. Zheng. This work was supported in part by grants from Science Foundation Ireland (02-IN1-B266), the National Institutes of Health (R01 program: GM61070 and GM75915; the NIH Roadmap Initiative: P50 GM073197; and the Protein Structure Initiative: U54 GM074961) and the National Science Foundation (IIS-0308078).

Published online at <http://www.natureprotocols.com>  
Reprints and permissions information is available online at <http://npg.nature.com/reprintsandpermissions>

1. Laver, W.G., Bischofberger, N. & Webster, R.G. Disarming flu viruses. *Sci. Am.* **280**, 78–87 (1999).
2. Renfrey, S. & Featherstone, J. Structural proteomics. *Nat. Rev. Drug Discov.* **1**, 175–176 (2002).
3. Caffrey, M. Membrane protein crystallization. *J. Struct. Biol.* **142**, 108–132 (2003).
4. Wiener, M.C. A pedestrian guide to membrane protein crystallization. *Methods* **34**, 364–372 (2004).
5. Sutton, B.J. & Sohi, M.K. Crystallization of membrane proteins for X-ray analysis. *Methods Mol. Biol.* **27**, 1–18 (1994).
6. Fromme, P. Crystallization of Photosystem I. In *Methods and Results in Crystallization of Membrane Proteins* (ed. Iwata, S.) 145–174 (International University Line, San Diego, 2003).
7. Ng, J.D., Stevens, R.C. & Kuhn, P. Protein crystallization in restricted geometry: advancing old ideas for modern times in structural proteomics. *Methods Mol. Biol.* **426**, 363–376 (2008).
8. Ng, J.D., Gavira, J.A. & Garcia-Ruiz, J.M. Protein crystallization by capillary counterdiffusion for applied crystallographic structure determination. *J. Struct. Biol.* **142**, 218–231 (2003).
9. Loll, P.J., Tretiakova, A. & Soderblom, E. Compatibility of detergents with the microbatch-under-oil crystallization method. *Acta Crystallogr. D Biol. Crystallogr.* **59**, 1114–1116 (2003).
10. Chayen, N.E. Crystallization of Membrane Proteins in Oils. In *Methods and Results in Crystallization of Membrane Proteins* (ed. Iwata, S.) 131–140 (International University Line, San Diego, 2003).

11. Raman, P., Cherezov, V. & Caffrey, M. The Membrane Protein Data Bank. *Cell. Mol. Life Sci.* **63**, 36–51 (2006).
12. Faham, S. & Bowie, J.U. Bicelle crystallization: a new method for crystallizing membrane proteins yields a monomeric bacteriorhodopsin structure. *J. Mol. Biol.* **316**, 1–6 (2002).
13. Takeda, K. *et al.* A novel three-dimensional crystal of bacteriorhodopsin obtained by successive fusion of the vesicular assemblies. *J. Mol. Biol.* **283**, 463–474 (1998).
14. Qiu, H. & Caffrey, M. The phase diagram of the monoolein/water system: metastability and equilibrium aspects. *Biomaterials* **21**, 223–234 (2000).
15. Luzzati, V. X-ray diffraction studies of lipid-water systems. In *Biological Membranes, Physical Fact and Function* Vol. 1, (ed. Chapman, D.) 71–123 (Academic Press, London, 1968).
16. Shipley, G.G., Green, J.P. & Nichols, B.W. The phase behavior of monogalactosyl, digalactosyl, and sulphoquinovosyl diglycerides. *Biochim. Biophys. Acta* **311**, 531–544 (1973).
17. Wisniewski, J.R. Protocol to enrich and analyze plasma membrane proteins from frozen tissues. *Methods Mol. Biol.* **432**, 175–183 (2008).
18. Yip, T.T. & Hutchens, T.W. Immobilized metal-ion affinity chromatography. *Methods Mol. Biol.* **244**, 179–190 (2004).
19. Selkirk, C. Ion-exchange chromatography. *Methods Mol. Biol.* **244**, 125–131 (2004).
20. Cutler, P. Size-exclusion chromatography. *Methods Mol. Biol.* **244**, 239–252 (2004).
21. Landau, E.M. & Rosenbusch, J.P. Lipidic cubic phases: a novel concept for the crystallization of membrane proteins. *Proc. Natl. Acad. Sci. USA* **93**, 14532–14535 (1996).
22. Cherezov, V., Clogston, J., Papiz, M.Z. & Caffrey, M. Room to move: crystallizing membrane proteins in swollen lipidic mesophases. *J. Mol. Biol.* **357**, 1605–1618 (2006).
23. Cherezov, V. *et al.* In meso structure of the cobalamin transporter, BtuB, at 1.95  $\text{\AA}$  resolution. *J. Mol. Biol.* **364**, 716–734 (2006).
24. Cherezov, V. *et al.* In meso crystal structure and docking simulations suggest an alternative proteoglycan binding site in the OpcA outer membrane adhesin. *Proteins* **71**, 24–34 (2008).
25. Cherezov, V. *et al.* High-resolution crystal structure of an engineered human beta2-adrenergic G protein-coupled receptor. *Science* **318**, 1258–1265 (2007).



26. Jaakola, V.P. *et al.* The 2.6 angstrom crystal structure of a human A2A adenosine receptor bound to an antagonist. *Science* **322**, 1211–1217 (2008).
27. Cherezov, V. & Caffrey, M. Nano-volume plates with excellent optical properties for fast, inexpensive crystallization screening of membrane proteins. *J. Appl. Cryst.* **36**, 1372–1377 (2003).
28. Cherezov, V., Peddi, A., Muthusubramaniam, L., Zheng, Y.F. & Caffrey, M. A robotic system for crystallizing membrane and soluble proteins in lipidic mesophases. *Acta Crystallogr. D Biol. Crystallogr.* **60**, 1795–1807 (2004).
29. Cherezov, V. & Caffrey, M. Picolitre-scale crystallization of membrane proteins. *J. Appl. Cryst.* **39**, 604–606 (2006).
30. Cherezov, V. & Caffrey, M. A simple and inexpensive nanoliter-volume dispenser for highly viscous materials used in membrane protein crystallization. *J. Appl. Cryst.* **38**, 398–400 (2005).
31. Ai, X. & Caffrey, M. Membrane protein crystallization in lipidic mesophases: detergent effect. *Biophys. J.* **79**, 394–405 (2000).
32. Misquitta, Y. & Caffrey, M. Detergents destabilize the cubic phase of monoolein: implications for membrane protein crystallization. *Biophys. J.* **85**, 3084–3096 (2003).
33. Cheng, A., Hummel, B., Qiu, H. & Caffrey, M. A simple mechanical mixer for small viscous lipid-containing samples. *Chem. Phys. Lipids* **95**, 11–21 (1998).
34. Lide, D.R. (ed.). *CRC Handbook of Chemistry and Physics* 89th edn. (CRC Press, Boca Raton, FL, 2008).
35. Misquitta, Y. *et al.* Rational design of lipid for membrane protein crystallization. *J. Struct. Biol.* **148**, 169–175 (2004).
36. Lunde, C.S. *et al.* UV microscopy at 280 nm is effective in screening for the growth of protein microcrystals. *J. Appl. Cryst.* **38**, 1031–1034 (2005).
37. Ng, J.D. *et al.* The crystallization of biological macromolecules from precipitates: evidence for Ostwald ripening. *J. Cryst. Growth* **168**, 50–62 (1996).
38. Benvenuti, M. & Mangani, S. Crystallization of soluble proteins in vapor diffusion for x-ray crystallography. *Nat. Protoc.* **2**, 1633–1651 (2007).
39. Nollert, P. & Landau, E.M. Enzymic release of crystals from lipidic cubic phases. *Biochem. Soc. Trans.* **26**, 709–713 (1998).
40. Luecke, H., Schobert, B., Richter, H.T., Cartailier, J.P. & Lanyi, J.K. Structure of bacteriorhodopsin at 1.55 Å resolution. *J. Mol. Biol.* **291**, 899–911 (1999).
41. Pflugrath, J.W. Macromolecular cryocrystallography—methods for cooling and mounting protein crystals at cryogenic temperatures. *Methods* **34**, 415–423 (2004).
42. Liu, W. & Caffrey, M. Gramicidin structure and disposition in highly curved membranes. *J. Struct. Biol.* **150**, 23–40 (2005).
43. Taylor, R., Burgner, J.W., Clifton, J. & Cramer, W.A. Purification and characterization of monomeric *Escherichia coli* vitamin B12 receptor with high affinity for colicin E3. *J. Biol. Chem.* **273**, 31113–31118 (1998).
44. Papiz, M.Z. *et al.* Crystallization and characterization of two crystal forms of the B800–850 light-harvesting complex from *Rhodospseudomonas acidophila* strain 10050. *J. Mol. Biol.* **209**, 833–835 (1989).
45. Prince, S.M. *et al.* Expression, refolding and crystallization of the OpcA invasin from *Neisseria meningitidis*. *Acta Crystallogr. D Biol. Crystallogr.* **57**, 1164–1166 (2001).
46. Rosenbaum, D.M. *et al.* GPCR engineering yields high-resolution structural insights into beta2-adrenergic receptor function. *Science* **318**, 1266–1273 (2007).
47. Cherezov, V. & Caffrey, M. Membrane protein crystallization in lipidic mesophases. A mechanism study using X-ray microdiffraction. *Faraday Discuss.* **136**, 195–212 (2007).
48. Cherezov, V., Fersi, H. & Caffrey, M. Crystallization screens: compatibility with the lipidic cubic phase for *in meso* crystallization of membrane proteins. *Biophys. J.* **81**, 225–242 (2001).
49. Caffrey, M. Kinetics and mechanism of transitions involving the lamellar, cubic, inverted hexagonal, and fluid isotropic phases of hydrated monoacylglycerides monitored by time-resolved X-ray diffraction. *Biochemistry* **26**, 6349–6363 (1987).
50. Cherezov, V. *et al.* Biophysical and transfection studies of the diC(14)-amidine/DNA complex. *Biophys. J.* **82**, 3105–3117 (2002).
51. Blanton, T.N. *et al.* JCPDS—International Centre for Diffraction Data round robin study of silver behenate. A possible low-angle X-ray diffraction calibration standard. *Powder Diffr.* **10**, 91–95 (1995).
52. Zhu, T. & Caffrey, M. Thermodynamic, thermomechanical, and structural properties of a hydrated asymmetric phosphatidylcholine. *Biophys. J.* **65**, 939–954 (1993).
53. Cherezov, V., Riedl, K.M. & Caffrey, M. Too hot to handle? Synchrotron X-ray damage of lipid membranes and mesophases. *J. Synchrotron Radiat.* **9**, 333–341 (2002).
54. Lakowicz, J. *Principles of Fluorescence Spectroscopy* (Plenum Press, New York, 1983).
55. Caffrey, M. & Feigenson, G.W. Fluorescence quenching in model membranes. 3. Relationship between calcium adenosinetriphosphatase enzyme activity and the affinity of the protein for phosphatidylcholines with different acyl chain characteristics. *Biochemistry* **20**, 1949–1961 (1981).
56. Misquitta, L.V. *et al.* Membrane protein crystallization in lipidic mesophases with tailored bilayers. *Structure* **12**, 2113–2124 (2004).
57. Cherezov, V., Clogston, J., Misquitta, Y., Abdel-Gawad, W. & Caffrey, M. Membrane protein crystallization *in meso*: lipid type-tailoring of the cubic phase. *Biophys. J.* **83**, 3393–3407 (2002).